



UNIVERSITÀ DI PARMA

ARCHIVIO DELLA RICERCA

University of Parma Research Repository

Redox-Switchable Calix[6]arene-Based Isomeric Rotaxanes

This is the peer reviewed version of the following article:

Original

Redox-Switchable Calix[6]arene-Based Isomeric Rotaxanes / Zanichelli, Valeria; Bazzoni, Margherita; Arduini, Arturo; Franchi, Paola; Lucarini, Marco; Ragazzon, Giulio; Secchi, Andrea; Silvi, Serena. - In: CHEMISTRY-A EUROPEAN JOURNAL. - ISSN 0947-6539. - 24:(2018), pp. 12370-12382. [10.1002/chem.201800496]

Availability:

This version is available at: 11381/2849067 since: 2021-01-29T19:59:32Z

Publisher:

Wiley-VCH Verlag

Published

DOI:10.1002/chem.201800496

Terms of use:

Anyone can freely access the full text of works made available as "Open Access". Works made available

Publisher copyright

note finali coverpage

(Article begins on next page)

02 May 2026

Molecular Machines



Redox-Switchable Calix[6]arene-Based Isomeric Rotaxanes

Valeria Zanichelli,^[a] Margherita Bazzoni,^[a] Arturo Arduini,^[a] Paola Franchi,^[b] Marco Lucarini,^[b] Giulio Ragazzon,^{*[b, c]} Andrea Secchi,^{*[a]} and Serena Silvi^{*[b]}

Abstract: Operating molecular machines are based on switchable systems whose components can be set in motion in a controllable fashion. The presence of nonsymmetrical elements is a mandatory requirement to obtain and demonstrate the unidirectionality of motion. Calixarene-based macrocycles have proved to be very efficient hosts in the design of oriented rotaxanes and of pseudorotaxanes with strict control over the direction of complexation. A series of two-station rotaxanes based on bipyridinium–ammonium axles was synthesized and characterized. A recently reported su-

pramolecularly assisted strategy for the synthesis of different orientational isomers was exploited, and the ammonium unit was identified as a proper secondary station for the calixarene. Displacement of the macrocycle was triggered by electrochemical reduction of the bipyridinium primary station, and it was shown that the shuttling is influenced both by the length of the chain of the axle component and by the position of the secondary station with respect to the calixarene rims.

Introduction

In the field of molecular-level machines, the possibility to synthesize and operate supramolecular systems capable of performing specific movements under the action of a defined external energy input is a fascinating challenge.^[1–5] One of the simplest classes of molecular machines is represented by molecular shuttles based on rotaxane architectures, which were first characterized by Stoddart et al. in solution in 1991.^[6] Since that report, many mechanically interlocked molecules have been designed, synthesized, and shown to mimic the complex functions of macroscopic switches with a wide range of applications, including molecular electronic devices, sensors, nanomechanical systems, and instruments capable of delivering both chemical and biological cargos in a controlled manner.^[7–10] The shuttling motion can be triggered by a ple-

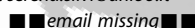
thora of different stimuli,^[4,11] such as thermal treatment,^[12] ion coordination,^[13,14] electrochemical^[15] or photochemical^[16,17] activation, and changes of solvent or pH.^[18] To obtain work from a molecular machine, and to move from switches to real molecular motors, full control over the direction of motion must be attained.^[19–22] This is one of the main challenges when designing a molecular machine and it involves the exploitation of inherently nonsymmetrical components, arranged in univocally oriented architectures. Indeed, asymmetry is a fundamental factor in the majority of systems reported to date, not only for obtaining unidirectionality of motion, but also for demonstrating it.^[23]

In a rotaxane-based architecture, asymmetry can be included in both the axle and wheel components. The majority of two-station molecular shuttles reported so far is based on nonsymmetrical axles,^[18,24,25] but in principle the direction of motion in a rotaxane could be dictated by the asymmetry of the wheel component (Figure 1).^[22,26–31] In a minimalistic design like that shown in Figure 1a, on weakening the interaction between the axle and the ring the formation of two orientational isomers could be envisaged. If the nonsymmetrical ring has a preferential direction of motion, dictated by the different natures of its two rims, then it would be possible to get selectively only one orientational isomer. If both the axle and the ring are nonsymmetrical (Figure 1b), then two orientational isomers can be synthesized, and the movement of the ring can give rise to four translational isomers (Figure 1b).

We have exploited the complexation abilities of calix[6]arene derivative **Cx** (Figure 2) toward 4,4'-bipyridinium-based axles^[32,33] to synthesize nonsymmetrical rotaxanes. In these systems, both the axle and the wheel components are nonsymmetrical (Figure 1b):^[33] the calixarene has two rims, which are functionalized with three *N*-phenylureido groups (upper rim)

[a] Dr. V. Zanichelli, M. Bazzoni, Prof. A. Arduini, Prof. A. Secchi
Dipartimento di Scienze Chimiche, della Vita e della
Sostenibilità Ambientale, Università di Parma
Parco Area delle Scienze 17/A, 43124 Parma (Italy)
E-mail: andrea.secchi@unipr.it

[b] Dr. P. Franchi, Prof. M. Lucarini, Dr. G. Ragazzon, Dr. S. Silvi
Dipartimento di Chimica "G. Ciamician", Università di Bologna
Via Selmi 2, 40126 Bologna (Italy)
E-mail: serena.silvi@unibo.it



[c] Dr. G. Ragazzon
Dipartimento di Scienze Chimiche, Università di Padova
via Marzolo 1, 35131, Padova (Italy)
E-mail: giulio.ragazzon@unipd.it

The ORCID numbers for the authors of this article can be found under:
<https://doi.org/10.1002/chem.201800496>.

Part of a Special Issue to commemorate young and emerging scientists. To view the complete issue, visit Issue 47.

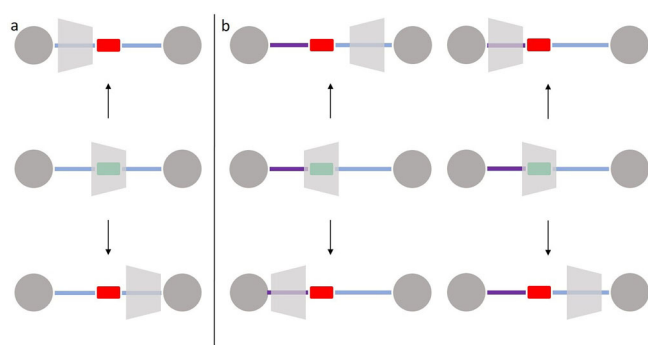


Figure 1. Rotaxanes with a) a symmetrical axle and a nonsymmetrical ring and b) two nonsymmetrical components (two orientational isomers): on weakening the interaction between the axle and the ring, different translational isomers can be obtained, depending on the direction of motion of the ring.

and three octyl chains (lower rim) and differ in both size and chemical properties, and the dumbbells are decorated with two alkyl chains with an appropriate difference in length. Moreover, in each molecule, the components are arranged in a univocal and controlled relative orientation, giving rise to con-

stitutionally isomeric oriented rotaxanes. Since the functionalized calixarene is nonpalindromic, the movement of the wheel towards one side of the axle would be chemically nonequivalent to that towards the opposite side and could therefore generate specific translational isomers (Figure 1b). We first planned to induce shuttling by exploiting the response of these redox-active systems to electrochemical stimulation.^[33] However, it emerged that electrochemical reduction of the bipyridinium core alone is not sufficient to induce any mechanical rearrangement in these rotaxanes. Cyclic voltammetry and EPR measurements showed that, contrarily to what was observed for similar pseudorotaxane assemblies,^[34] no detectable movement of the macrocyclic component takes place when the axle is mechanically interlocked in a rotaxane-type structure,^[32] regardless of the nature and the orientation of the threaded dumbbell.^[33] From these results, it emerged that the presence of a further recognition element is mandatory to facilitate displacement and promote shuttling. We thus focused our attention on two-station rotaxanes, equipped with two distinct recognition sites (stations) on their dumbbell-shaped component, in which the macrocycle can move from one site to the other in a controlled and reversible manner. To achieve this goal, it is crucial that the two stations exhibit different association strengths with the receptor. If this is the case, the rotaxane can exist as two different equilibrating co-conformations, the populations of which reflect their relative free energies, determined by the extent of the two different sets of noncovalent bonding interactions. To this end, in this work we tackled the synthesis of a series of two-station rotaxanes constituted by the calix[6]arene wheel **Cx** and dialkylviologen-based axles endowed with an ammonium station as second recognition unit on the dumbbell (Figure 2).

Results and Discussion

Synthesis of rotaxanes

To describe the results of this study, we labeled the compounds with descriptors showing (Figure 2): 1) the position of the ammonium station with respect to the rims of the calix-

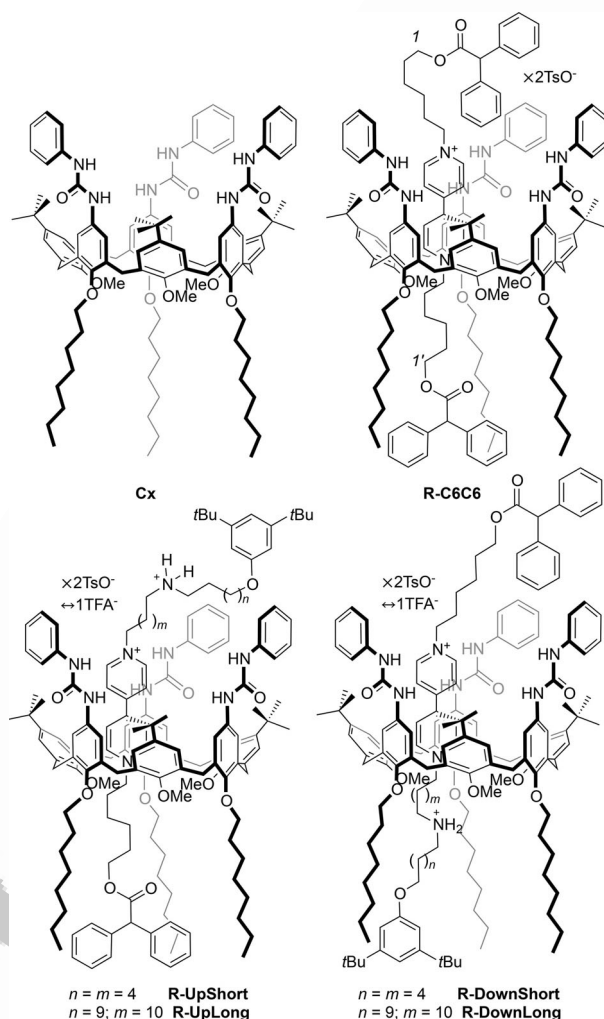
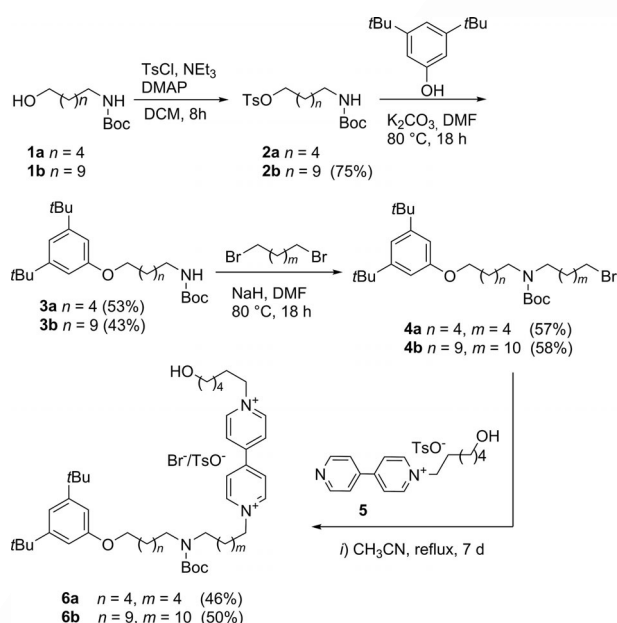


Figure 2. One- and two-station rotaxanes derived from calix[6]arene **Cx**.

Giulio Ragazzon pursued his Master degree as a student of Collegio Superiore, the Excellence Institution of Bologna University. He obtained his PhD in 2017 at the same university, under the supervision of Prof. Credi. He is now a postdoctoral fellow at the University of Padova with Prof. Prins. In his career, he spent research periods abroad in UK, France, and Japan. His research started in photochemistry and moved to molecular machines and supramolecular systems, with a fascination for nonequilibrium phenomena. He received several prizes, remarkably the gold medal at the 2016 European Young Chemist Award (PhD level). This would not have been possible without excellent co-workers and collaborators.



ene (**Up** if the station is oriented towards the upper rim, **Down** if it is oriented towards the lower rim), 2) the length of the N-containing side chain connected to the pyridinium nitrogen atom (**Long** or **Short**). Labels **DB**, **P**, and **R** denote, dumbbells pseudorotaxanes, and rotaxanes, respectively. To gain information about a possible preferential shuttling direction, pivoted by the inherent asymmetry of **Cx**, we designed two different series of orientational rotaxane isomers in which the ammonium station (N-station) faces the two opposite rims of the macrocycle. To have insight into the influence of the length of the spacers and to assure that the movement is not impeded by neighboring molecular components, each series was synthesized with a long (C₁₂NC₁₁) and a short (C₆NC₆) side chain (Figure 2). Taking inspiration from previous protocols,^[33] we designed the synthesis of axles endowed with a bulky stopper at one end and a terminal OH group at the opposite side. For the preparation of the rotaxanes having the longer N-containing side chain toward the calixarene upper rim, the appropriate *N*-Boc-protected axles **6a** and **6b** were synthesized according to Scheme 1. *N*-Boc-protected ω-aminoalcohols **1a,b** were con-

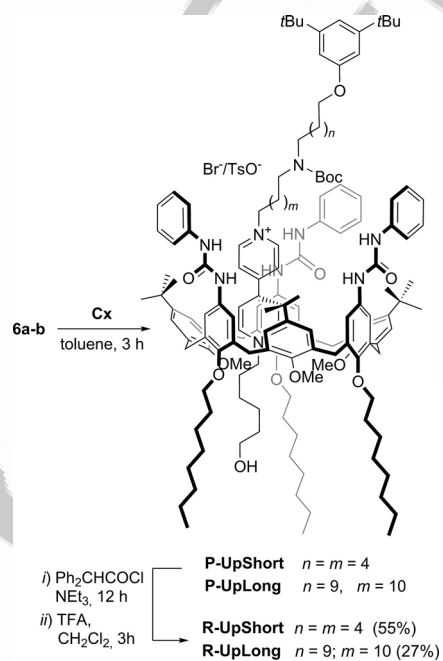


Scheme 1. Synthesis of *N*-Boc-protected axles **6a** and **6b**. Boc = *tert*-butoxycarbonyl, DMAP = 4-dimethylaminopyridine.

verted to tosylates **2a,b**, which were first treated with 3,5-*di-tert*-butylphenol in the presence of K₂CO₃ to insert the stopper (**3a,b**) and then with a molar excess of 1,6-dibromohexane or 1,12-dibromododecane to complete the backbone of the N-containing alkyl side chains. Reaction of the resulting bromides **4a,b** with pyridyl pyridinium tosylate **5** finally afforded axles **6a** and **6b** in 46 and 50% yield, respectively (see Experimental Section).

In separate experiments, these axles were then equilibrated at room temperature in toluene with an equivalent of wheel **Cx**. After stirring for 3 h at room temperature, the initial suspensions gradually turned homogeneous and red-colored. This

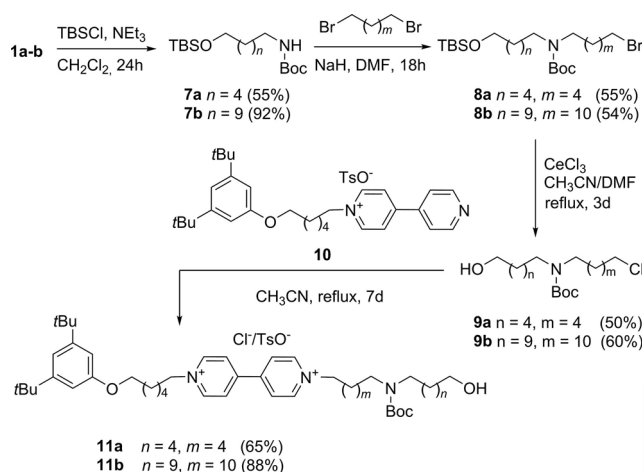
coloration is usually ascribed to the charge-transfer interaction occurring in a pseudorotaxane complex between the viologen core of the axle and the π-rich aromatic cavity of the calixarene. As shown in previous studies,^[35,36] the presence on the axle of a terminal bulky stopper leads to unidirectional threading of the axle from the upper rim of **Cx** with its ω-hydroxyhexyl chain and thus to the exclusive formation of oriented pseudorotaxanes **P-UpShort** and **P-UpLong**, as depicted in Scheme 2. The subsequent axle stoppering reaction with di-



Scheme 2. Synthesis of target rotaxanes **R-UpShort** and **R-UpLong**.

phenylacetyl chloride, carried out directly in the toluene solution of each pseudorotaxane, followed by treatment with trifluoroacetic acid of the dichloromethane solutions of the resulting *N*-Boc-protected rotaxanes, allowed us to eventually isolate the desired rotaxanes **R-UpShort** and **R-UpLong** in 55 and 27% overall yield, respectively (see Scheme 2).

For the preparation of the orientational rotaxane isomers having the N-station facing the lower rim of the calixarene wheel (**R-DownLong** and **R-DownShort** in Figure 2), we designed the synthesis of axles **11a** and **11b**, which are endowed with a secondary ammonium group between the viologen unit and the terminal OH group (see Scheme 3). In the first step, the hydroxyl group of **1a,b** was protected with *tert*-butyldimethylsilyl chloride (TBSCl), and then the Boc-protected NH group of the resulting doubly protected derivatives **7a,b**, was alkylated with the appropriate α,ω-dibromoalkane to yield amines **8a,b**. In the following step, all attempts to free the OH group of these derivatives through cleavage of the silyl ether group with tetrabutylammonium fluoride led to an undesired fluoro/bromo exchange. Finally, deprotection with anhydrous CeCl₃ afforded chlorides **9a,b** having a terminal hydroxyl moiety and a suitable leaving group (Cl) for alkylation of bipyridine. These compounds were treated in refluxing acetonitrile with pyridyl



Scheme 3. Synthesis of *N*-Boc-protected axles **11a** and **11b**.

pyridinium salt **10**, functionalized with a stoppered C₆ alkyl chain, to afford axles **11a** and **11b** in 65 and 88% yield, respectively (see Experimental Section).

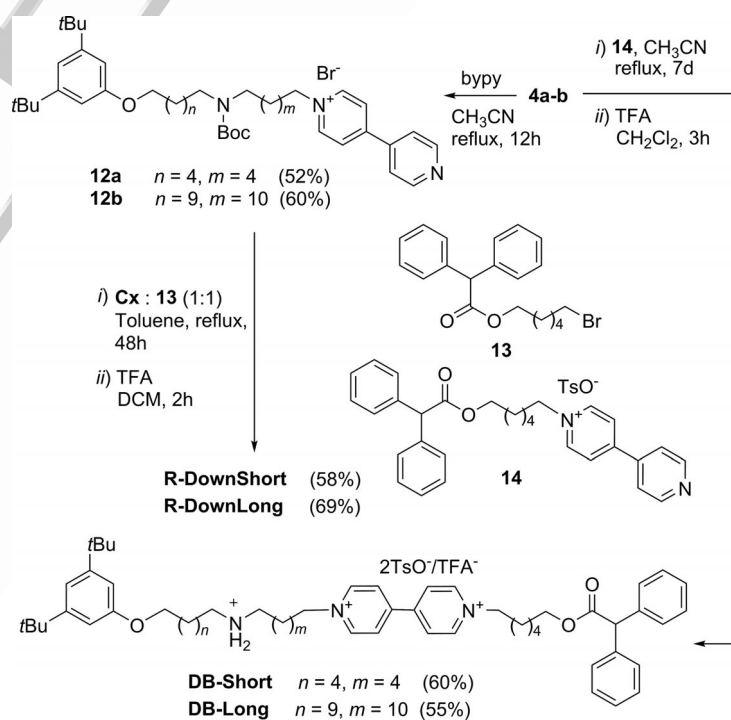
In separate experiments, **11a** and **11b** were then suspended in toluene and mixed with an equimolar amount of wheel **Cx**. In these two reactions, no hints of complexation were observed: the heterogeneous mixture never turned homogeneous and the supernatant toluene solution remained uncolored. Heating the two mixtures to reflux for several hours did not change the result. The ESI-MS analysis of the reaction mixtures (carried out in MeOH to provide solubility of the axle) revealed the sole presence of the unchanged reagents, that is, no side reaction or reagent degradation took place; in fact, after chromatographic separation, **Cx** was recovered almost quantitatively.

The impossibility to obtain any pseudorotaxane complex through these reactions was mainly ascribed to the bulkiness of the protected secondary amine in **11a** and **11b**, which prevents threading of the axle bearing the carbamate moiety in proximity to the lower rim of the wheel. Overall, the above threading-and-capping sequential strategy has shown the remarkable advantages of complete selectivity in the synthesis of orientational isomers in which the *N*-station faces the upper rim of the calix[6]arene: **R-UpShort** and **R-UpLong** (Figure 2). On the other hand, its major drawback is the impossibility to obtain assemblies having bulky moieties arranged downward or in nonlinear conformations, because such dumbbells cannot efficiently thread the wheel component.

To overcome these limitations, we envisaged investigating whether the recent results we obtained in the supramolecularly assisted synthesis of oriented calix[6]arene-based rotaxanes^[37,38] can be extended to the preparation of rotaxanes that cannot be synthesized by traditional procedures. In this recent work, it was indeed shown that the alkylation of pyridyl pyridinium salts such as **5** and **10** in presence of

an analogue of **Cx** takes place preferentially inside the calix[6]-arene cavity with the non-alkylated pyridine ring facing the calixarene upper rim. This alkylation gives thus rise to the formation of pseudorotaxane structures. If a bulky terminal group is present on the alkyl chain of the pyridyl pyridinium guest, the following assisted alkylation and stoppering reactions lead to the formation of oriented rotaxanes in which the alkyl chain initially appended to the pyridinium group, regardless of its length, is located close to the lower rim of the wheel.^[37,38]

Starting from these results, we therefore designed the synthesis of stoppered pyridyl pyridinium salts having the Boc-protected *N*-station between the phenolic stopper and pyridyl pyridinium moiety and alkyl spacers between the amino group and the two opposite ends of different length. In separate experiments, **4a,b** were first treated with a large excess of 4,4'-bipyridine in refluxing acetonitrile (see Scheme 4), and the resulting pyridyl pyridinium salts **12a** and **12b**, easily isolated by filtration, were then mixed in toluene with equimolar amounts of **Cx** and **13**. The latter compound is a C₆ alkylating agent mono-stoppered with a bulky diphenylacetic moiety. These supramolecularly assisted rotaxation reactions went to completeness after 2 d of heating to reflux (solutions turned homogeneous and red-colored). After chromatographic separation, the rotaxanes were immediately treated with TFA in dichloromethane to deprotect the *N*-station. After solvent removal, the oriented rotaxanes **R-DownShort** and **R-DownLong** were obtained in 58 and 69% overall yield. Model dumbbell compounds **DB-Long** and **DB-Short** were synthesized as depicted in Scheme 4.



Scheme 4. Supramolecularly assisted synthesis of rotaxanes **R-DownShort** and **R-DownLong** and synthesis of dumbbells **DB-Short** and **DB-Long**. TFA = trifluoroacetic acid.

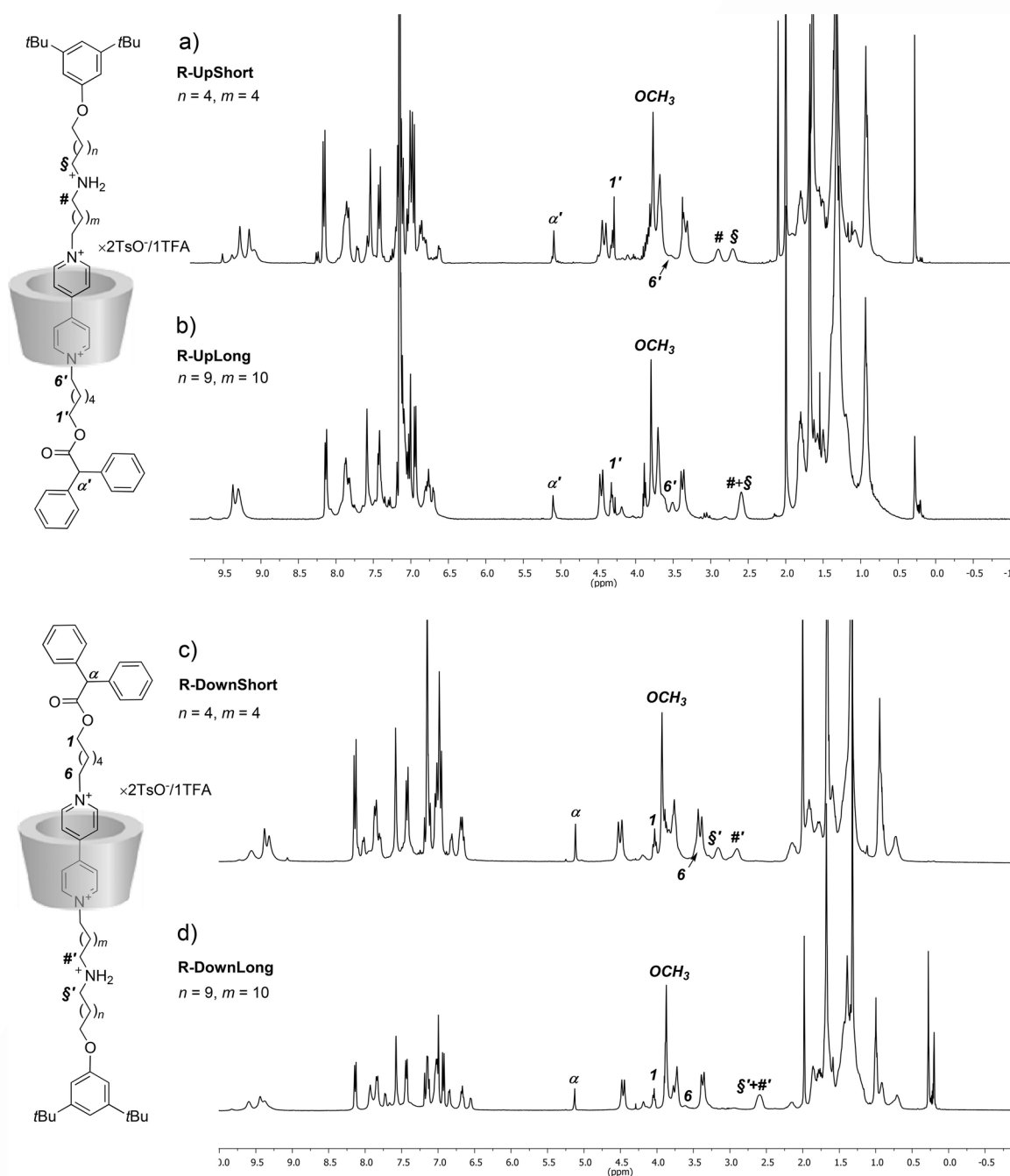


Figure 3. ^1H NMR stack plots (C_6D_6 , 400 MHz) of the series of two-station rotaxanes (the most-diagnostic signals are indicated in sketches on the left).

Characterization of rotaxanes

The inclusion of a bipyridinium-based dumbbell in a calix[6]arene wheel can be assessed through analysis of the chemical shifts of some diagnostic proton signals.^[32,33,36,39–41] The presence of a single sharp signal at about 3.8 ppm for the lower-rim methoxyl groups confirms the presence of a single orientational isomer in solution (Figure 3). Considering the cone shape adopted by the calix[6]arene cavity on threading and its extension due to the three *N*-phenylurea units at its upper rim, it is known that all signals of the stoppered alkyl chain facing the phenylurea groups are further shifted upfield than those belonging to the opposite side chain.^[32,33,35,36] To assess the ori-

entation of the unsymmetrical dumbbells **DB-Short** and **DB-Long** with respect to the rims of the wheel, we took advantage of our previous NMR studies carried out on a symmetrical rotaxane bearing two C_6 alkyl chains at the opposite sides of the bipyridinium station, **R-C6C6** (see Figure 2),^[32] which shares with the two-station rotaxanes so far synthesized the same alkylated bipyridinium moiety with a diphenylacetic stopper. In this rotaxane, the methylene group nearby the diphenylacetic stopper, indicated with the label *1* or *1'* depending on the orientation of its hexyl chain with respect to the asymmetric aromatic cavity (upper and lower rim, respectively, see Figure 2), is greatly affected by changes of the magnetic environment. It

gives rise to two well-separated NMR signals at $\delta = 4.38$ and 4.08 ppm (see Table 1, entry 1), and the more strongly upfield shifted one relative to the methylene group (1) of the hexyl chain is located toward the wheel upper rim (see Figure 2).^[32]

Table 1. ¹H NMR chemical shifts (δ , ppm, C₆D₆, 400 MHz) of the most diagnostic methylene signals of the dumbbell in the series of two-station rotaxanes **R-Down** and **R-Up**. The chemical shift of the same signals for symmetric rotaxane **R-C6C6** are reported for comparison.^[a,b]

Rotaxane	Chemical shift [ppm]					
	1'	1	#'	#	§'	§
R-C6C6	4.38	4.08	-	-	-	-
R-UpShort	4.31	-	-	2.9	-	2.7
R-UpLong	4.32	-	-	2.6	-	2.6
R-DownShort	-	4.03	2.9	-	3.2	-
R-DownLong	-	4.04	2.6	-	2.6	-
DB-Long		4.17			3.0 ^[c]	
DB-Short		4.16			3.0 ^[c]	

[a] For the assignment of NMR signals, see Figure 3. [b] A prime label indicates the orientation of the methylene group toward the lower rim of the wheel. [c] In the noncomplexed dumbbells these signals overlap.

Through simple comparison of the chemical shifts of these signals, it was then possible to foresee that the side chain containing the N-station in **R-UpShort** and **R-UpLong** (see Figure 3a,b and Table 1) is oriented toward the upper rim of the wheel. The same applies for rotaxanes **R-DownShort** and **R-DownLong**, in which the N-station is oriented in the opposite direction (see Figure 3c,d and Table 1). In the two short rotaxane isomers **R-UpShort** and **R-DownShort**, characterized by an N-containing side chain with short spacers, also the signals of the two methylene groups near the ammonium moiety are affected by the orientation of the dumbbell inside **Cx**. In **R-UpShort** these methylene groups resonate as two broad signals at $\delta = 2.9$ and 2.7 ppm, labeled, respectively as # and § (see Figure 3a). In the opposite orientational isomer **R-DownShort**, one of these two signals (§') is downfield-shifted at $\delta = 3.2$ ppm (see Figure 3c). In the longer dumbbell of the rotaxane isomers **R-UpLong** and **R-DownLong**, both methylene groups give rise to a unique broad signal centered at about 2.6 ppm regardless of their position with respect to the cavity. This is coherent with the increased distance of the ammonium group (C₁₂ spacer) from the cavity in these two rotaxanes. Moreover, for each rotaxane, 2D NMR measurements (COSY, TOCSY, NOESY, HSQC) were carried out to facilitate complete characterization of the products. The formation of the two-station rotaxanes was also confirmed by HRMS (see Experimental Section).

Electrochemical behavior of rotaxanes

Parent pseudorotaxanes composed of a bipyridinium-based axle and a tris-phenylureido calix[6]arene can be operated by means of electrochemical stimulation, that is, electrochemical reduction of the bipyridinium unit to its radical cation causes dethreading of the molecular components.^[34] On the other

hand, in rotaxanes lacking a second recognition unit for the calixarene, reduction of the bipyridinium ring does not displace the ring from the station.^[32,33] The response of the two-station rotaxanes to electrochemical stimulation was steered through cyclic voltammetry (CV) and differential pulse voltammetry (DPV) measurements in acetonitrile, and the measured potentials were compared to those of uncomplexed dumbbells **DB-Long** and **DB-Short** (see Table 2). For the sake of compari-

Table 2. Electrochemical potentials (vs. SCE) of the investigated compounds. Conditions: argon-purged acetonitrile, 0.04 M tetraethylammonium hexafluorophosphate, 300–400 μ M analyte.

Species	Reduction potentials [V]	
	E ₁	E ₂
DOV	-0.42 ^[42]	-0.87 ^[42]
DB-Short	-0.41	-0.85
DB-Long	-0.40	-0.85
R-UpShort	-0.60	-0.94
R-UpLong	-0.61	-0.87
R-DownShort	-0.52	-0.93
R-DownLong	-0.60	-0.88
R-C6C6	-0.64 ^[32,33]	-1.15 ^[32,33]

son, the reduction potentials of the 1,1'-dioctyl-4,4-bipyridinium (**DOV**) axle and of symmetric rotaxane **R-C6C6** are also reported. In line with previously analyzed systems, all compounds show two reversible or quasireversible monoelectronic reduction processes.^[32] The reduction potentials of the two dumbbells are similar to those of **DOV**, and thus demonstrate that the electrochemical properties of the bipyridinium moiety are not influenced by the stoppers or by the ammonium units.

As expected, the first reduction potential of each two-station rotaxane isomer is shifted towards more negative values with respect to the corresponding free axle in solution, and lies at almost the same potential as in model compound **R-C6C6** (Figure 4), as a consequence of the stabilization of the bipyridi-

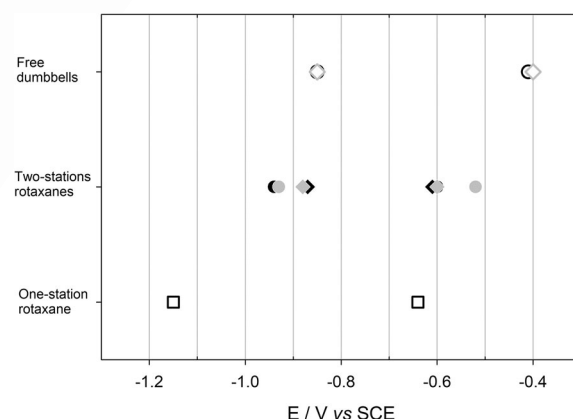


Figure 4. Measured reduction potentials of the studied compounds: dumbbells **DB-Short** (empty circles) and **DB-Long** (empty diamonds), two-station rotaxanes **R-UpLong** (black diamonds), **R-DownLong** (gray diamonds), **R-UpShort** (black circles), **R-DownShort** (gray circles), and one-station rotaxane **R-C6C6** (empty squares).

nium unit induced by the calixarene cavity.^[32–34] On the other hand, the second reduction potentials are comparable to those of uncomplexed dumbbells (Figure 4). These results, together with the EPR data (vide infra), indicate that the calixarene ring moves away from the monoreduced bipyridinium unit. Nevertheless, the reversibility of the first reduction waves in the cyclic voltammogram suggests that the shuttling equilibria in the monoreduced state are fast with respect to the scanning speed. The scan rates explored with our apparatus did not evidence any dependence of the peak position and separation on the scan rate, but digital simulations of the experiments and fitting of the experimental data confirmed our hypothesis.

The voltammetric curves obtained for rotaxane **R-UpShort** were fitted according to the scheme shown in Figure 5, by fixing the reduction potentials for the encapsulated and free species to the experimental values. The vertical processes are the electrochemical reactions, whereas the horizontal processes are the shuttling reactions. The values of the thermodynamic constants for these equilibria are also reported. Closer inspection of the reduction potentials (Figure 4) suggests a dependence both on the length of the N-containing alkyl chains (short or long) and on the position of the ammonium site with respect to the calixarene rims (up or down). The analysis of the second reduction potentials shows that the reduction of the rotaxanes with shorter chains **R-UpShort** and **R-DownShort**, bearing the ammonium unit closer to the macrocycle, is slightly more difficult (regardless of the orientation of the calix[6]arene) with respect to the reduction of the long isomers; this result suggests that a weak but non-negligible interaction between the calixarene and the monoreduced bipyridinium unit is still present in the short isomers, in agreement with EPR results (vide infra).

This finding would also suggest that when the ammonium group is close to the bipyridinium unit, it is possible for the calixarene macrocycle to interact with both sites simultaneously, regardless of the orientation of the axle. This observation is somewhat surprising, because the two rims of the calix[6]arene are different from a chemical point of view, and it is therefore not easy to imagine different interaction modes that result in

very similar interaction energies. The analysis of the first reduction potential also reveals a dependence on the relative orientation of the axle and the ring. Rotaxane **R-DownShort**, with a short N-containing chain close to the lower rim of the calixarene, is easier to reduce with respect to all the other rotaxanes. This would suggest that the calixarene is less engaged in charge-transfer interactions with the bipyridinium unit, possibly because it is involved in the interaction with the ammonium site already in the oxidized form, besides in the monoreduced state, as suggested by EPR data (vide infra). This hypothesis is also supported by the reversed position of the NMR signals of **R-DownShort** and **R-UpShort** (vide supra).

EPR measurements on rotaxanes

The hypothesis of a shuttling motion of Cx was also supported by the EPR spectra of uncomplexed dumbbells and rotaxanes recorded after electrochemical reduction in deoxygenated acetonitrile at room temperature. The EPR spectra of the bipyridinium radical cations $\text{bpy}^{\bullet+}$ obtained by one-electron reduction are shown in Figure 6. According to previous studies on the radical cations of 1,1'-dialkyl-4,4'-bipyridinium derivatives,^[33] all the spectra can be well reproduced by assuming coupling of the unpaired electron with two equivalent N atoms and three groups of four equivalent protons: one group is due to the methylene groups of the two chains, and the other two equivalent sets arise from the aromatic protons. By using the above spectral pattern all the spectra can be nicely reproduced with the hyperfine splitting constants reported in Table 3. In all cases, the *g* factors were close to 2.0031. According to the literature,^[33] the smaller hyperfine coupling constant for H atoms was assigned to the aromatic α protons, whereas the larger coupling was attributed to the methylene groups of the two alkyl chains. Inspection of these data clearly shows that: 1) EPR parameters of the monoreduced two-station rotaxanes are similar to those measured for the uncomplexed monoreduced dumbbells **DB-Short**⁺ and **DB-Long**⁺ (Figure 6); 2) the values of the hyperfine coupling constants are consistent with a symmetrical distribution of the two aromatic rings of the bipyridine unit. We have already shown that trapping $\text{bpy}^{\bullet+}$ in the

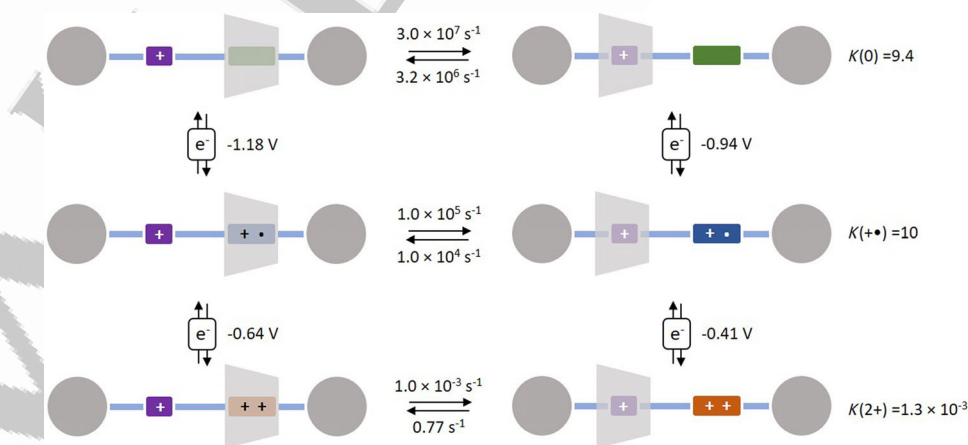


Figure 5. Reaction scheme showing the thermodynamic and kinetic data for the simulated voltammogram of **R-UpShort**. Reduction potentials partly taken from refs. [32] and [33].

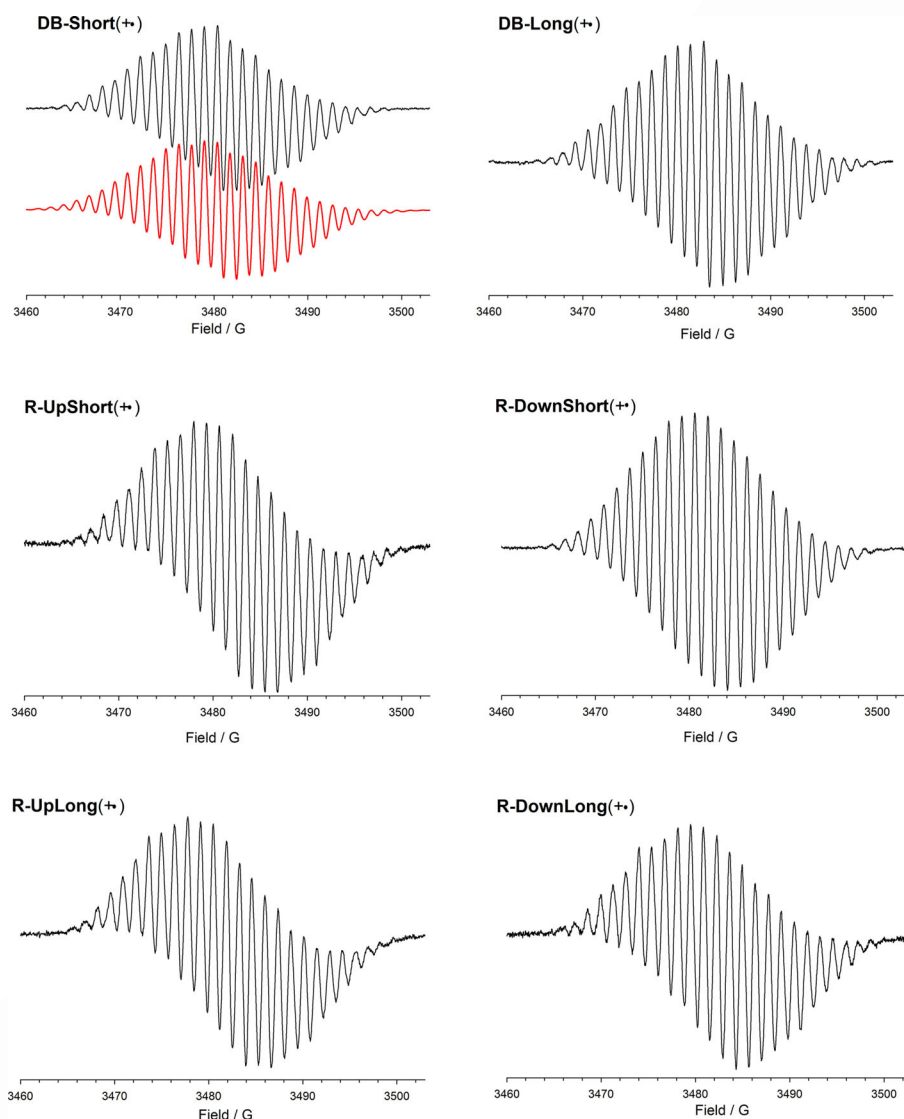


Figure 6. EPR spectra (recorded in acetonitrile) of electrochemically reduced noncomplexed dumbbells and two-station rotaxanes.

Table 3. EPR hyperfine splitting constants a [Gauss] of radical cations obtained after electrochemical reduction of the bipyridinium unit at room temperature in CH_3CN .

	$a_{2\text{N}}$	$a_{2\text{CH}_2}$	$a_{4\text{H}\beta}$	$a_{4\text{H}\alpha}$
DB-Short ⁺	4.10	4.06	1.61	1.11
DB-Long ⁺	4.13	4.05	1.58	1.12
R-UpShort ⁺	4.16	3.98	1.66	1.20
R-DownShort ⁺	4.17	4.11	1.47	1.30
R-UpLong ⁺	4.13	4.01	1.62	1.17
R-DownLong ⁺	4.14	4.04	1.61	1.15

asymmetric wheel of **Cx** induces a nonsymmetrical distribution of the spin density in the two heterocyclic rings.^[33] Thus, the present results suggest that bpy^+ does not interact significantly with the calix[6]arene cavity in all derivatives, irrespective of the length of the alkyl chains on the axle and the relative position of the two components of the rotaxane.

The hyperfine splitting constants measured in the EPR spectrum of the short rotaxane radical cations **R-UpShort⁺** and **R-DownShort⁺** which are slightly different to those measured with the noncomplexed dumbbells and long rotaxane radical cations deserve a brief comment. Actually, these small differences suggest that it is possible for the aromatic or aliphatic tails of the calix[6]arene to maintain a weak but non-negligible interaction with the monoreduced bipyridinium unit when the ammonium recognition site is close to the bipyridinium unit. In conclusion, EPR results, in agreement with the electrochemical data, confirm that the addition of one electron to the bipyridinium site induces the displacement of the wheel away from it.

Conclusions

The design, synthesis, and structural characterization of new oriented two-station calix[6]arene-based rotaxanes have been presented. Several challenges in the field of calixarene-based

molecular machines have been tackled. First, two different procedures were used for the synthesis of the two orientational isomers. The **Up** isomers, bearing an ammonium station in proximity to the upper rim of the wheel, were synthesized by a traditional sequential threading-and-capping procedure; the **Down** isomers, in which the second recognition unit faces the lower part of the wheel, were obtained by exploiting a supramolecularly assisted strategy that was recently reported.^[37,38] Moreover, we have demonstrated that the ammonium moiety can play the role of a secondary station for the calixarene and the ability of these systems to behave as molecular shuttles driven by electrochemical stimulation. Voltammetric and EPR measurements evidenced that, on the first mono-electronic reduction of the bipyridinium unit of the axle, rearrangement of the systems takes place. This indicates that, coherently with our initial hypothesis, the electrochemical input induces shuttling of the calixarene towards the more favored second recognition site, and the complete reduction of the radical cation to its neutral form takes place outside the calixarene cavity. Finally, we have observed dependence of the shuttling both on the length of the chain of the axles and on the relative orientation of the molecular components. On the basis of the collected data, in a symmetrical rotaxane bearing a central bipyridinium unit and two peripheral ammonium stations connected by short spacers, reduction of the electroactive unit is expected to induce shuttling of the calixarene preferentially towards the ammonium station located at its lower rim, that is, a directional motion would be dictated only by the orientation of the wheel on a symmetrical axle. Three-station rotaxanes based on these architectures are currently under investigation in our laboratories.

Experimental Section

Synthesis and characterization

Toluene, THF, acetonitrile, and dichloromethane were dried by following standard procedures; other reagents were of reagent-grade quality, obtained from commercial sources, and used without further purification. Chemical shifts are expressed in ppm with the residual solvent signal as internal reference. Mass spectra were determined in ESI mode. Compounds **1a**,^[43] **1b**,^[44] **2a**,^[43] **7a**,^[45] **13**,^[35] **5**,^[43] **10**,^[46] **14**,^[33] **R-C6C6**,^[32] axle **DOV**,^[34] and wheel **Cx**^[47] were synthesized according to reported procedures.

tert-Butyl-N-[11-[(4-methylbenzenesulfonyl)oxy]undecyl]carbamate (2b): Triethylamine (1.7 g, 17.9 mmol), tosyl chloride (3 g, 15.8 mmol), and a catalytic amount of DMAP were added in this order to a solution of **1b** (3.5 g, 12.2 mmol) in dry dichloromethane (50 mL). After stirring at room temperature for 24 h, the reaction was quenched with water (50 mL). The separated organic phase was dried over anhydrous CaCl₂, filtered, and the solvent evaporated to dryness under reduced pressure. The sticky residue was purified by column chromatography (*n*-hexane/ethyl acetate 85:15) to afford **2b** as a white solid (75%); m.p. 57–59 °C; ¹H NMR (400 MHz, CDCl₃): δ = 1.2–1.4 (m, 14H), 1.47 and 1.4–1.5 (s, m, 11H), 1.6–1.7 (m, 2H), 2.47 (s, 3H), 3.11 (brs, 2H), 4.04 (t, *J* = 6.5 Hz, 2H), 4.5 (brs, 1H), 7.36 (d, *J* = 7.6 Hz, 2H), 7.81 ppm (d, *J* = 7.6 Hz, 2H); ¹³C NMR (100 MHz, CDCl₃): δ = 21.6, 25.3, 26.8, 28.4, 28.8, 28.9, 29.2, 29.3 (2 res.), 29.4, 30.0, 40.6, 70.7, 78.8, 127.8, 129.8, 133.2,

144.6, 156.2 ppm; ESI-MS(+) *m/z* (%) [ion]: 464 (100) [*M*+Na]⁺; elemental analysis (%) calcd for C₂₃H₃₀NO₅S: C 62.55, H 8.90, N 3.17; found: C 62.61.43, H 8.95, N 2.99%.

General procedure for the synthesis of 3a,b: Tosylate **2a** or **2b** (7 mmol) was added to a solution of 3,5-di-*tert*-butylphenol (6.3 mmol) and K₂CO₃ (2.6 g, 18.8 mmol) in dry DMF (50 mL). The resulting reaction mixture was stirred at 80 °C for 12 h. After cooling to room temperature, the reaction was quenched with water (50 mL) and extracted with ethyl acetate (3 × 100 mL). The separated organic phase was dried with Na₂SO₄ and evaporated to dryness under reduced pressure.

tert-Butyl N-[6-(3,5-di-*tert*-butylphenoxy)hexyl]carbamate (3a): The residue was purified by column chromatography (*n*-hexane/acetone 85:15) to afford **3a** as a colorless oil (53%); ¹H NMR (400 MHz, CDCl₃): δ = 1.33 (s, 18H), 1.4–1.6 and 1.47 (2 m, s, 15H), 1.8–1.9 (m, 2H), 3.14 (t, *J* = 6.7 Hz, 2H), 3.98 (t, *J* = 6.4 Hz, 2H), 4.5 (brs, 1H), 6.77 (s, 2H), 7.03 ppm (s, 1H); ¹³C NMR (100 MHz, CDCl₃): δ = 25.9, 26.6, 28.5, 29.4, 30.1, 31.5, 35.0, 40.6, 67.5, 77.2, 108.8, 114.8, 152.1, 156.0, 158.6 ppm; ESI-MS(+) *m/z* (%) [ion]: 428 (100) [*M*+Na]⁺.

tert-Butyl N-[11-(3,5-di-*tert*-butylphenoxy)undecyl]carbamate (3b): The residue was purified by column chromatography (*n*-hexane/THF 85:15) to afford **3b** as a colorless oil (43%); ¹H NMR (400 MHz, CDCl₃): δ = 1.2–1.4 and 1.33 (m, s, 30H), 1.4–1.5 (m, 13H), 1.8–1.9 (m, 2H), 3.12 (t, *J* = 6.4 Hz, 2H), 3.98 (t, *J* = 6.4 Hz, 2H), 4.51 (brs, 1H), 6.78 (s, 2H), 7.03 ppm (s, 1H); ¹³C NMR (75 MHz, CDCl₃): δ = 26.1, 26.8, 28.4, 29.3, 29.5 (3 res.), 29.6, 30.1, 30.3, 31.5, 35.0, 40.6, 72.9, 79.1, 108.8, 114.7, 152.1, 156.0, 158.7 ppm; ESI-MS(+) *m/z* (%) [ion]: 499 (100) [*M*+Na]⁺.

General procedure for the synthesis of 4a,b: NaH (0.2 g of a 60% dispersion in mineral oil, ca. 5 mmol) was slowly added to a solution of *N*-protected amine **3a** or **3b** (2.5 mmol) in dry DMF (50 mL), kept under inert atmosphere and cooled at 0 °C through an external ice bath. The resulting reaction mixture was stirred at room temperature for 3 h, then cooled again at 0 °C, and the appropriate α,ω-dibromoalkane (7.5 mmol) was added dropwise. After stirring for 18 h at room temperature, the reaction mixture was carefully quenched with water (40 mL) and extracted with ethyl acetate (3 × 50 mL). The organic phase was dried over Na₂SO₄ and evaporated under reduced pressure.

tert-Butyl N-(6-bromohexyl)-N-[6-(3,5-di-*tert*-butylphenoxy)hexyl]carbamate (4a): The residue was purified by column chromatography (*n*-hexane/THF 95:5) to afford **4a** as a colorless oil (0.75 g, 57%); ¹H NMR (400 MHz, CDCl₃): δ = 1.33 (s, 18H) 1.4–1.6 and 1.48 (m, s, 21H), 1.8–1.9 (m, 4H), 3.1–3.2 (m, 4H), 3.42 (t, *J* = 6.8 Hz, 2H), 3.98 (t, *J* = 6.4 Hz, 2H), 6.77 (d, *J* = 1.6 Hz, 2H), 7.03 ppm (t, *J* = 1.6 Hz, 1H); ¹³C NMR (100 MHz, CDCl₃): δ = 26.0, 26.1, 26.7, 28.0, 28.5, 30.0, 31.5, 32.8, 33.8, 35.0, 46.9, 47.0, 67.6, 79.0, 108.8, 114.8, 152.1, 155.6, 158.6 ppm; ESI-MS(+) *m/z* (%) [ion]: 590 (95), 591 (25), 592 (100) [*M*+Na]⁺.

tert-Butyl N-(12-bromododecyl)-N-[11-(3,5-di-*tert*-butylphenoxy)undecyl]carbamate (4b): The residue was purified by column chromatography (*n*-hexane/THF 95:5) to afford **4b** as a colorless oil (1.35 g, 58%). ¹H NMR (400 MHz, CDCl₃): δ = 1.2–1.4 and 1.34 (m, s, 44H), 1.4–1.5 (m, 17H), 1.8–1.9 (2 m, 4H), 3.2 (brs, 4H), 3.43 (t, *J* = 6.8 Hz, 2H), 3.98 (t, *J* = 6.5 Hz, 2H), 6.78 (d, *J* = 1.6 Hz, 2H), 7.03 ppm (t, *J* = 1.6 Hz, 1H); ¹³C NMR (100 MHz, CDCl₃): δ = 26.2, 26.9, 28.2, 28.5, 28.8, 29.4 (3 res.), 29.5 (4 res.), 29.6 (5 res.), 29.6, 30.4, 31.5, 32.9, 34.1, 35.0, 47.1, 67.8, 78.9, 108.8, 114.8, 152.1, 155.7, 158.7 ppm; ESI-MS(+) *m/z* (%) [ion]: 744 (90), 745 (40), 746 (98), 747 (45) [*M*+Na]⁺.

General procedure for the synthesis of axles 6a,b: In a sealed glass autoclave, a solution of salt **5** (0.14 g, 0.3 mmol) and the appropriate bromide (**4a** or **4b**, 0.6 mmol) in dry acetonitrile (5 mL) was heated to reflux for 7 d. After cooling to room temperature, the reaction mixture was refrigerated at 0 °C until precipitation of a yellow solid was observed.

Axle 6a: The yellow precipitate was collected by Buchner filtration and washed with cold acetonitrile (46%); m.p. 197–198 °C; ¹H NMR (300 MHz, CD₃OD): δ = 1.33 (s, 18H), 1.4–1.7 and 1.48 (m, s, 25H), 1.7–1.9 (m, 2H), 2.0–2.2 (m, 4H), 2.39 (s, 3H), 3.24 (t, *J* = 6.8 Hz, 4H), 3.60 (t, *J* = 6.2 Hz, 2H), 4.00 (t, *J* = 6.2 Hz, 2H), 4.78 (t, *J* = 7.5 Hz, 4H), 6.77 (s, 2H), 7.05 (s, 1H), 7.25 (d, *J* = 8 Hz, 2H), 7.70 (d, *J* = 8 Hz, 2H), 8.71 (d, *J* = 6.5 Hz, 4H), 9.30 ppm (d, *J* = 6.5 Hz, 4H); ¹³C NMR (75 MHz, CD₃OD): δ = 18.0, 23.8, 23.9, 24.1, 24.2, 24.4, 24.8, 26.0, 26.8, 27.2, 27.4, 27.7, 29.1, 29.6, 30.4, 32.9, 46.2, 59.8, 60.3, 65.8, 77.8, 107.1, 112.8, 124.1, 125.4, 127.1, 138.8, 140.9, 145.4, 148.3, 150.3, 154.5, 157.3 ppm; ESI-MS(+) *m/z* (%) [ion]: 744.5 (100) [M–H]⁺; elemental analysis (%) calcd for C₅₄H₈₂BrN₃O₇S: C 65.04, H 8.29, N 4.21; found: C 64.22.43, H 7.99, N 4.42%.

Axle 6b: The yellow precipitate was collected by Buchner filtration and washed with cold acetonitrile (50%); m.p. >300 °C decomp; ¹H NMR (400 MHz, CD₃OD): δ = 1.2–1.4 (m, 44H), 1.4–1.6 (m, 21H), 1.7–1.9 (m, 4H), 2.0–2.2 (m, 4H), 2.38 (s, 3H), 3.18 (t, *J* = 7.2 Hz, 4H), 3.58 (t, *J* = 6.4 Hz, 2H), 3.97 (t, *J* = 6.4 Hz, 2H), 4.76 (m, 4H), 6.74 (s, 2H), 7.02 (s, 1H), 7.24 (d, *J* = 8 Hz, 2H), 7.69 (d, *J* = 8 Hz, 2H), 8.69 (d, *J* = 6.4 Hz, 4H), 9.29 ppm (d, *J* = 6.4 Hz, 2H); ¹³C NMR (100 MHz, CD₃OD): δ = 20.0, 25.0, 25.6, 25.9 (2 res.), 26.5, 26.6, 27.5 (2 res.), 27.8 (2 res.), 28.3, 28.5, 28.8, 29.1, 29.2 (2 res.), 29.3, 29.4, 30.6, 31.1, 31.2, 31.8, 32.6, 33.1 (2 res.), 34.4, 46.7, 61.2, 61.8, 67.4, 79.2, 108.6, 114.3, 125.5, 126.9, 128.5, 140.3, 142.3, 145.7, 149.8, 151.7, 156.0, 158.8 ppm; ESI-MS(+) *m/z* (%) [ion]: 899.8 (100), 900.7 (65) [M–H]⁺; 1070.6 (25), 1071.8 (20) [M+TsO]⁺; elemental analysis (%) calcd for C₆₅H₁₀₄BrN₃O₇S: C 67.80, H 9.10, N 3.65; found: C 66.95, H 8.65, N 4.01%.

General procedure for the sequential synthesis of two-station rotaxanes R-UpShort and R-UpLong: The appropriate mono-stoppered axle (**6a** or **6b**, 0.06 mmol) was suspended in a solution of wheel **Cx** (0.09 g, 0.06 mmol) in anhydrous toluene (15 mL). The suspension was stirred at room temperature for 3 h until the solution turned homogeneous and dark red in color. Triethylamine (0.01 g, 0.1 mmol) and diphenylacetyl chloride (0.03 g, 0.1 mmol) were then added, and the resulting reaction mixture was stirred overnight at room temperature. After removing the solvent under reduced pressure, the solid residue was partitioned between dichloromethane and water. The organic phase was separated and evaporated under reduced pressure, and the crude product was purified by column chromatography (dichloromethane/methanol 50:1). The resulting *N*-Boc-protected rotaxane was then dissolved in anhydrous dichloromethane (10 mL) and trifluoroacetic acid (2 mL) was added dropwise. The solution turned yellow. After stirring at room temperature for 2 h, the solvent was evaporated under reduced pressure to afford the desired deprotected rotaxane.

R-UpShort: The product was isolated as a red solid (55%); m.p. >300 °C (decomp); ¹H NMR (400 MHz, C₆D₆): δ = 0.8 (brs, 2H), 0.8–1.0 (m, 17H), 1.1 (brs, 6H), 1.2–1.4 and 1.33 (brs, s, 68H), 1.5–1.7 and 1.64 (brs, s, 46H), 1.8 (brs, 12H), 1.9 (brs, 2H), 2.00 (s, 12H), 2.10 (s, 4H), 2.7 (brs, 2H), 2.9 (brs, 2H), 3.2–3.4 (m, 8H), 3.5–3.7 (2 brs, 12H), 3.7–3.9 and 3.77 (m, s, 12H), 4.31 (t, *J* = 6.0 Hz, 2H), 4.42 (d, *J* = 12.0 Hz, 6H), 5.09 (s, 1H), 6.59 (d, *J* = 5.2 Hz, 2H), 6.7 (brs, 2H), 6.9 (brs, 3H), 7.0 (brs., 14H), 7.2 (brs, 11H), 7.42 (d, *J* = 7.2 Hz, 4H), 7.54 (s, 6H), 7.70 (d, *J* = 5.2 Hz, 2H), 7.83 (d, *J* = 6.8 Hz, 6H), 8.2 (brs, 2H), 8.23 (d, *J* = 8.0 Hz, 4H), 9.0–9.3 ppm (m,

7H); ¹³C NMR (100 MHz, C₆D₆): δ = 13.2, 20.0, 21.9, 24.6, 25.0, 25.2, 25.6, 25.7, 26.2, 27.1, 27.2, 28.3, 28.7, 28.8, 28.9, 29.9, 30.7, 31.1, 33.8, 33.9, 47.9, 48.2, 56.4, 59.8, 59.9, 60.3, 61.1, 62.8, 64.0, 66.5, 72.3, 108.3, 113.6, 115.8, 117.3, 120.4, 124.0, 124.8, 125.1, 125.7, 126.4, 126.7, 127.0, 127.3, 127.7 (2 res.), 127.8, 128.0, 128.5, 128.6, 131.2, 132.8, 136.5, 138.2, 138.6, 140.3, 142.1, 142.5, 143.5, 145.3, 147.5, 151.1, 152.0, 152.5, 158.6, 171.1 ppm; HRMS calcd for C₁₅₈H₂₀₉N₉O₁₂: *m/z* = 1212.3005 [M]²⁺; found: 1212.3027.

R-UpLong: The product was isolated as a red solid (27%); m.p. >300 °C dec.; ¹H NMR (400 MHz, C₆D₆): δ = 0.6–1.0 (m, 9H), 1.1–1.3 (m, 57H), 1.4–1.6 (m, 12H), 1.69 (s, 18H), 1.8 (brs, 4H), 1.99 (s, 6H), 2.59 (brs, 4H), 3.38 (d, *J* = 14.4 Hz, 6H), 3.5 (brs, 4H), 3.7 (brs, 6H), 3.79 (s, 9H), 3.88 (t, *J* = 7.0 Hz, 2H), 4.32 (t, *J* = 6.8 Hz, 2H), 4.46 (d, *J* = 14.4 Hz, 6H), 5.11 (s, 1H), 6.9 (d, *J* = 5.2 Hz, 2H), 6.77 (t, *J* = 6.8 Hz, 3H), 6.83 (d, *J* = 5.2 Hz, 2H), 6.94 (d, *J* = 8.0 Hz, 4H), 7.0 (m, 4H), 7.15 (m, 7H), 7.43 (m, 4H), 7.59 (s, 6H), 7.82 (s, 6H), 7.88 (d, *J* = 5.2 Hz, 2H), 8.14 (d, *J* = 8.0 Hz, 4H), 9.2–9.4 ppm (m, 7H); ¹³C NMR (100 MHz, C₆D₆): δ = 14.0, 20.8, 22.8, 25.7 (2 res.), 25.8 (2 res.), 26.1 (2 res.), 26.4, 26.5, 26.6 (2 res.), 26.7, 28.8, 29.1, 29.2, 29.5 (2 res.), 29.6, 29.7 (2 res.), 29.8 (2 res.), 30.7, 30.8, 31.3, 31.5, 31.6, 31.9, 32.0 (2 res.), 34.6, 34.7, 38.2, 47.4, 47.5, 57.2, 59.7, 60.8, 64.8, 67.5, 73.1, 109.2, 114.4, 116.6, 118.1, 121.2, 124.8, 125.6, 126.4, 127.2, 128.3, 128.4, 128.5, 128.6, 128.7, 128.8, 129.3, 131.7, 132.0, 133.6, 137.3, 139.0, 139.6, 141.2, 142.9, 143.1, 144.1, 148.2, 148.4, 151.9, 152.9, 153.3, 159.5 ppm; HRMS calcd for C₁₆₉H₂₃₁N₉O₁₂: *m/z* = 1289.3866 [M]²⁺; found: 1289.3859.

tert-Butyl *N*-[11-[(tert-butyl)dimethylsilyloxy]undecyl] carbamate (7b): *tert*-Butylchlorodimethylsilane (0.89 g, 5.9 mmol) was slowly added to a solution of **1b** (1.4 g, 5 mmol) and triethylamine (0.6 g, 6 mmol) in dry dichloromethane (100 mL). A catalytic amount of DMAP was added. After stirring at room temperature for 2 h, the reaction was quenched with water (50 mL) and the organic phase was separated, washed with brine, dried over anhydrous CaCl₂ and filtered. The solvent was removed under reduced pressure to afford **7b** as a colorless oily residue (92%). ¹H NMR (400 MHz, CDCl₃): δ = 0.05 (s, 6H), 0.90 (s, 9H), 1.3–1.5 (m, 14H), 1.4–1.5 (m, 13H), 3.1 (brs, 2H), 3.60 (t, *J* = 6.8 Hz, 2H), 4.5 ppm (brs, 1H); ¹³C NMR (100 MHz, CDCl₃): δ = –5.3, 14.1, 18.4, 22.6, 25.7, 25.8, 26.0, 26.8, 28.4, 29.3, 29.4, 29.5 (2 res.), 29.6, 30.1, 31.6, 32.9, 40.7, 63.3, 78.9, 156.0 ppm; ESI-MS(+) *m/z* (%) [ion]: 424 (100), 425 (30) [M+Na]⁺.

General procedure for the synthesis of 8a,b: NaH (0.35 g of a 60% dispersion in mineral oil, ca. 9 mmol) was slowly added to a solution of the appropriate *N*-protected amine (**5a** or **5b**, 4.4 mmol) in dry DMF (50 mL), kept under inert atmosphere and cooled at 0 °C through an external ice bath. The resulting reaction mixture was stirred at room temperature for 3 h, and then cooled again at 0 °C and the appropriate α,ω-dibromoalkane (17.4 mmol) was added dropwise. After stirring for 24 h at room temperature, the reaction mixture was carefully quenched with water (100 mL) and extracted with ethyl acetate (3×50 mL). The organic phase was dried over Na₂SO₄ and evaporated under reduced pressure.

tert-Butyl *N*-(6-bromohexyl)-*N*-[6-[(tert-butyl)dimethylsilyloxy]hexyl] carbamate (8a): The residue was purified by column chromatography (*n*-hexane/THF 9:1) to afford **8a** as a colorless oil (1.19 g, 55%). ¹H NMR (400 MHz, CDCl₃): δ = 0.009 (s, 6H), 0.86 (s, 9H), 1.2–1.3 (m, 4H), 1.42 (s, 9H), 1.4–1.5 (m, 10H), 1.8–1.9 (m, 2H), 3.1 (brs, 4H), 3.36 (t, *J* = 7 Hz, 2H), 3.56 ppm (t, *J* = 8 Hz, 2H); ¹³C NMR (100 MHz, CDCl₃): δ = –5.26, 14.1, 18.4, 22.7, 25.6, 25.9, 26.1, 26.7, 28.0, 29.7, 30.3, 32.8, 33.8, 46.8, 47.0, 63.2, 79.0, 155.6 ppm; ESI-MS(+) *m/z* (%) [ion]: 516 (100), 518 (97), 519 (30) [M+Na]⁺.

tert-Butyl N-(12-bromododecyl)-N-([11-(tert-butylidimethylsilyloxy)undecyl] carbamate (8b): The residue was purified by column chromatography (*n*-hexane/THF 98:2) to afford **8b** as a colorless oil (2.52 g, 54%). ¹H NMR (300 MHz, CDCl₃): δ = 0.06 (s, 6H), 0.91 (s, 9H), 1.2–1.3 (m, 28H), 1.46 (s, 9H), 1.4–1.6 (m, 8H), 1.8–1.9 (m, 2H), 3.15 (t, *J* = 7 Hz, 4H), 3.42 (t, *J* = 6.8 Hz, 2H), 3.61 ppm (t, *J* = 6.6 Hz, 2H); ¹³C NMR (100 MHz, CDCl₃): δ = -5.3, 25.8, 26.0, 26.9, 28.2, 28.5, 28.8, 29.4, 29.5, 29.6, 32.8, 32.9, 34.0, 47.0, 63.3, 78.8, 155.6 ppm; ESI-MS(+) *m/z* (%) [ion]: 648 (95), 650 (100), 651 (40) [M+H]⁺.

General procedure for the synthesis of 9a,b: Anhydrous cerium(III) chloride (3.1 mmol) was added to a solution of bromide **8a** or **8b** (1.6 mmol) in a mixture of dry acetonitrile (80 mL) and DMF (10 mL). The reaction mixture was heated to reflux for 3 d. The solution was then cooled to room temperature and the solvent removed under reduced pressure. The oily residue was extracted with ethyl acetate (100 mL) and washed with water (3 × 50 mL). The separated organic phase was dried over Na₂SO₄ and evaporated under reduced pressure.

tert-Butyl N-(6-chlorohexyl)-N-(6-hydroxyhexyl) carbamate (9a): The crude product was purified by column chromatography (*n*-hexane/THF 6:4) to afford chlorinated product **9a** as a colorless oil (50%). ¹H NMR (400 MHz, CDCl₃): δ = 1.3–1.4 (m, 4H), 1.47 (s, 9H), 1.4–1.6 (m, 8H), 1.6 (brs, 2H), 1.8–1.9 (m, 2H), 3.2 (brs, 4H), 3.55 (t, *J* = 6.4 Hz, 2H), 3.65 ppm (t, *J* = 6 Hz, 2H); ¹³C NMR (100 MHz, CDCl₃): δ = 26.2, 26.7, 28.5, 31.0, 32.6, 32.7, 45.0, 46.8, 62.6, 62.9, 79.1, 155.7 ppm; ESI-MS(+) *m/z* (%) [ion]: 336 (100), 338 (30), 337 (20) [M+H]⁺; 358 (100), 360 (30) 359 (20) [M+Na]⁺; 374 (100), 376 (30), 375 (20) [M+K]⁺.

tert-Butyl N-(12-chlorododecyl)-N-(11-hydroxyundecyl) carbamate (9b): The crude product was purified by column chromatography (*n*-hexane/ethyl acetate 9:1) to afford **9b** as a colorless oil (0.22 g, 60%). ¹H NMR (400 MHz, CDCl₃): δ = 1.2–1.3 (m, 28H), 1.45 (s, 9H), 1.4–1.6 (m, 8H), 1.7–1.8 (m, 2H), 3.13 (brs, 4H), 3.53 (t, *J* = 6.8 Hz, 2H), 3.63 ppm (t, *J* = 6.8 Hz, 2H); ¹³C NMR (100 MHz, CDCl₃): δ = 25.7, 26.9, 28.5, 28.9, 29.4 (2 res.), 29.5 (3 res.), 29.6, 32.6, 32.8, 45.1, 47.0, 63.0, 78.9, 155.7 ppm; ESI-MS(+) *m/z* (%) [ion]: 490 (100), 491 (30), 492 (30) [M+H]⁺; 512 (100), 513 (30), 514 (30) [M+Na]⁺; 528 (100), 529 (30), 530 (20) [M+K]⁺.

General procedure for the synthesis of axles 11a and 11b: Compound **10** (0.092 g, 0.15 mmol) and the appropriate chloride **9a** or **9b** (0.3 mmol) were dissolved in dry acetonitrile (5 mL) and the solution placed in a glass autoclave. After sealing the autoclave under inert atmosphere, the resulting reaction mixture was heated to reflux with stirring for 7 d. After this period, the reaction mixture was cooled to room temperature, diluted with 10 mL of ethyl acetate, and then placed in a refrigerator at 0 °C to promote the precipitation of the desired axle.

Axle 11a: A sticky white solid was collected by Buchner filtration and washed with cold ethyl acetate (65%). ¹H NMR (400 MHz, CD₃OD): δ = 1.3–1.6 (m, 36H), 1.83 (t, *J* = 6.8 Hz, 2H), 2.14 (t, *J* = 7.2 Hz, 4H), 2.37 (s, 6H), 3.1–3.2 (m, 4H), 3.5–3.6 (m, 2H), 3.99 (t, *J* = 6.0 Hz, 2H), 4.76 (t, *J* = 7.2 Hz, 4H), 6.74 (s, 2H), 7.03 (s, 1H), 7.24 (d, *J* = 8 Hz, 4H), 7.70 (d, *J* = 8 Hz, 4H), 8.66 (d, *J* = 6.0 Hz, 4H), 9.27 ppm (d, *J* = 6.0 Hz, 4H); ¹³C NMR (100 MHz, CD₃OD): δ = 19.9, 25.3, 25.6, 26.3, 27.4, 28.9, 30.5, 31.1, 32.2, 34.4, 61.2, 61.4, 61.8, 67.0, 79.3, 108.5, 114.4, 125.6, 126.9, 128.5, 140.3, 145.7, 149.9, 151.9, 156.0, 158.7, 160.7 ppm; ESI-MS(+) *m/z* (%) [ion]: 745 (100), 746 (50), 747 (20) [M–H]⁺; elemental analysis (%) calcd for C₅₄H₈₂ClN₃O₇S: C 68.07, H 8.68, N 4.41. Found: C 67.91, H 8.32, N 4.05%.

Axle 11b: A sticky yellow solid was collected by Buchner filtration (88%). ¹H NMR (400 MHz, CD₃OD): δ = 1.3–1.6 (m, 67H), 1.8–1.9 (m, 2H), 2.1–2.2 (m, 4H), 2.39 (s, 3H), 3.19 (t, *J* = 7.6 Hz), 3.55 (t, *J* = 6.8 Hz, 2H), 4.00 (t, *J* = 6.4 Hz, 2H), 4.8 (m, 4H), 6.75 (s, 2H), 7.02 (s, 1H), 7.25 (d, *J* = 8 Hz, 2H), 7.72 (d, *J* = 8 Hz, 2H), 8.71 (d, *J* = 6.4 Hz, 4H), 9.3 ppm (m, 4H); ¹³C NMR (100 MHz, CD₃OD): δ = 25.6, 25.9, 26.5 (2 res.), 27.4, 28.8, 28.9, 29.1, 29.2, 29.3, 30.5, 31.1, 31.2, 32.3, 34.4, 61.6, 61.8, 61.9, 67.1, 79.2, 108.6, 125.6, 127.1, 128.5, 140.3, 142.1, 145.7, 149.8, 151.8, 156.1, 158.8 ppm; ESI-MS(+) *m/z* (%) [ion]: 900 (100) [M–H]⁺; elemental analysis (%) calcd for C₆₅H₁₀₄ClN₃O₇S: C 70.52, H 9.47, N 3.80. Found: C 69.77, H 9.12, N 3.15%.

General procedure for the synthesis of 12a and 12b: Bromide **4a** or **4b** (0.3 mmol) and 4,4'-bipyridyne (1.0 mmol) were dissolved in dry acetonitrile (50 mL) and the solution heated to reflux overnight. The solvent was then removed under reduced pressure to afford a crude solid residue, which was triturated with ethyl acetate and hexane (4 × 25 mL).

1-(6-(6-(3,5-di-tert-butylphenoxy)hexyl)(tert-butoxycarbonyl)amino)hexyl)-4,4'-bipyridin-1-ium bromide (12a): After suction filtration **12a** was obtained as a sticky yellow solid (52%). ¹H NMR (300 MHz, CD₃OD): δ = 1.30 (s, 18H), 1.30–1.6 (m, 21H), 1.78 (t, *J* = 7.5 Hz, 2H), 2.19 (t, *J* = 6.8 Hz, 2H), 3.22 (t, *J* = 7.3 Hz, 4H), 3.97 (t, *J* = 7.5 Hz, 2H), 4.75 (t, *J* = 6.8 Hz, 4H), 6.73 (s, 2H), 7.01 (s, 1H), 8.04 (d, *J* = 8 Hz, 2H), 8.56 (d, *J* = 8 Hz, 2H), 8.84 (d, *J* = 8 Hz, 2H), 9.19 ppm (d, *J* = 8 Hz, 2H); ¹³C NMR (75 MHz, CD₃OD): δ = 25.6 (2 res.), 26.3, 27.5, 28.3, 29.1, 30.6, 31.0, 31.1, 34.4, 46.5, 61.9, 67.4, 79.3, 108.6, 114.3, 122.3, 125.8, 142.2, 145.2, 150.4, 151.8, 153.5, 156.0, 158.8 ppm; ESI-MS(+) *m/z* (%) [ion]: 645 (100), 646 (95), 647 (80) [M]⁺.

1-(12-(11-(3,5-di-tert-butylphenoxy)undecyl)(tert-butoxycarbonyl)amino)dodecyl)-4,4'-bipyridin-1-ium bromide (12b): After suction filtration **12b** was obtained as a sticky yellow solid (60%). ¹H NMR (400 MHz, CDCl₃): δ = 1.2–1.4 (m, 52H), 1.77 (t, *J* = 8 Hz, 2H), 2.08 (t, *J* = 7 Hz, 2H), 3.18 (t, *J* = 7.4 Hz, 4H), 3.97 (t, *J* = 8 Hz, 2H), 4.73 (t, *J* = 7 Hz, 2H), 6.73 (s, 2H), 7.02 (s, 1H), 8.03 (d, *J* = 8 Hz, 2H), 8.55 (d, *J* = 8 Hz, 2H), 8.85 (d, *J* = 8 Hz, 2H), 9.17 ppm (d, *J* = 8 Hz, 2H); ¹³C NMR (100 MHz, CDCl₃): δ = 25.8, 26.5 (2 res.), 27.5, 28.8, 29.1, 29.2 (2 res.), 29.3, 29.4, 30.6, 31.1, 34.4, 61.3, 67.5, 79.4, 108.6, 114.5, 122.4, 126.1, 142.2, 145.5, 150.5, 152.0, 153.7, 156.2, 159.1 ppm; ESI-MS(+) *m/z* (%) [ion]: 799 (100) 800 (80) 801 (40) [M]⁺.

General procedure for the supramolecularly assisted synthesis of Down rotaxanes: Wheel **Cx** (0.04 mmol), salt **12a** or **12b** (0.06 mmol), and bromide **13** (0.08 mmol) were suspended in dry toluene (15 mL), and the mixture was stirred for 2 d at 110 °C. After a few hours, the mixture turned red and homogeneous. The solvent was then removed under reduced pressure and the residue was partitioned between dichloromethane and water. The separated organic phase was evaporated under reduced pressure, and the crude product was purified by column chromatography (dichloromethane/methanol 50:1). The isolated Boc-protected rotaxane was then dissolved in 5 mL of dry dichloromethane and 5 mL of trifluoroacetic acid were added dropwise. The red solution turned yellow. After stirring at room temperature for 2 h, the solvent was evaporated under reduced pressure to give the deprotected rotaxane.

R-DownShort: The rotaxane was isolated as a red solid (0.06 g, 58%). M.p. > 300 °C (decomp); ¹H NMR (400 MHz, C₆D₆): δ = 0.76 (brs, 2H), 0.9–1.0 (m, 9H), 1.1–1.4 and 1.35 (m, s, 61H), 1.6 (m, 2H), 1.63 (s, 18H), 1.8 (brs, 2H), 1.9 (brs, 8H), 2.00 (s, 6H), 2.2 (brs, 4H), 2.9 (brs, 2H), 3.2 (brs, 2H), 3.4–3.5 (m, 8H), 3.8 (brs, 6H), 3.8 (brs, 2H), 3.9 (brs, 2H), 3.93 (s, 9H), 4.03 (t, *J* = 7.2 Hz, 2H), 4.50 (t, *J* =

15 Hz, 6H), 5.12 (s, 1H), 6.6–6.7 (m, 5H), 6.82 (d, $J=5.2$ Hz, 2H), 7.0 (brs, 11H), 7.2 (brs, 10H), 7.4–7.5 (m, 8H), 7.58 (s, 6H), 7.80 (d, $J=5.2$ Hz, 2H), 7.9 (brs, 6H), 8.03 (d, $J=5.2$ Hz, 2H), 8.14 (d, $J=8$ Hz, 4H), 9.2–9.6 ppm (m, 7H); ^{13}C NMR (100 MHz, C_6D_6): $\delta=14.1, 20.8, 22.8, 24.9, 25.5, 25.6, 25.9, 26.4, 26.7, 28.3, 29.3, 29.6, 29.8, 30.7, 31.3, 31.5, 32.0, 34.6, 34.8, 38.2, 46.8, 57.4, 60.5, 61.1, 64.7, 67.1, 73.3, 109.0, 114.8, 116.8, 118.1, 121.3, 124.8, 125.7, 126.4, 127.2, 128.6, 128.7$ (2 res.), 128.8129.3, 132.0, 133.6, 137.4, 139.2, 139.7, 141.1, 142.9, 143.2, 144.3, 146.3, 148.3, 148.4, 152.1, 152.8, 153.3, 159.2, 172.0 ppm; HRMS calcd for $\text{C}_{158}\text{H}_{209}\text{N}_9\text{O}_{12}$: $m/z=1212.3005$ $[\text{M}]^{2+}$; found: 1212.3013

R-DownLong: The product was isolated as a red solid (0.08 g, 69%). m.p. $>300^\circ\text{C}$ (decomp); ^1H NMR (400 MHz, C_6D_6): $\delta=0.7$ (brs, 2H), 0.9 (brs, 2H), 0.99 (t, $J=6$ Hz, 9H), 1.1–1.5 and 1.33 (m, s, 69H), 1.5–1.7 and 1.69 (m, s, 44H), 1.8 (brs, 4H), 1.9 (brs, 4H), 1.98 (s, 6H), 2.2 (brs, 2H), 2.6 (brs, 4H), 3.37 (d, $J=14.8$ Hz, 6H), 3.6 (brs, 2H), 3.7 (brs, 6H), 3.8 (brs, 2H), 3.9–4.0 (m, 11H), 4.04 (t, $J=6.8$ Hz, 2H), 4.47 (d, $J=14.8$ Hz, 6H), 5.13 (s, 1H), 6.55 (d, $J=5.2$ Hz, 2H), 6.68 (t, $J=7.2$ Hz, 3H), 6.85 (d, $J=5.2$ Hz, 2H), 6.93 (d, $J=8.4$ Hz, 4H), 7.0–7.1 (m, 8H), 7.12 (s, 1H), 7.1–7.2 and 7.19 (m, s, 8H), 7.44 (d, $J=7.2$ Hz, 6H), 7.58 (s, 6H), 7.72 (d, $J=5.2$ Hz, 2H), 7.8 (brs, 6H), 7.9 (brs, 4H), 8.14 (d, $J=8.4$ Hz, 4H), 9.3–9.6 ppm (m, 7H); ^{13}C NMR (100 MHz, C_6D_6): $\delta=14.1, 20.8, 22.8, 24.9, 25.5, 25.8, 26.4, 26.7$ (2 res.), 26.9, 28.0, 28.3, 28.6, 29.1, 29.2, 29.5, 29.6, 29.7 (3 res.), 29.8 (2 res.), 29.9, 30.0, 30.4, 30.6, 30.8, 31.2, 31.3, 31.5, 31.7, 32.0, 34.6, 34.8, 47.2 (2 res.), 57.4, 60.5, 60.8, 61.1, 64.6, 67.4, 73.0, 109.1, 114.6, 116.7, 118.0, 121.3, 124.7, 125.6, 125.4, 127.2, 127.6, 128.6, 128.7 (2 res.), 128.9, 129.3, 132.0, 133.7, 137.3, 139.2, 139.6, 141.0, 142.9, 143.1, 144.1, 147.9, 148.3, 152.0, 152.8, 153.2, 159.4, 172.0 ppm; HRMS calcd for $\text{C}_{169}\text{H}_{231}\text{N}_9\text{O}_{12}$: $m/z=1289.3866$ $[\text{M}]^{2+}$; found: 1289.3857.

General procedure for the synthesis of dumbbells DB-Short and DB-Long: Compound **14** (1 equiv) and the appropriate alkylating agent (**4a** for **DB-Short** or **4b** for **DB-Long**, 2 equiv) were dissolved in dry acetonitrile (20 mL) and the solution was placed in a glass autoclave. After sealing the autoclave under inert atmosphere, the resulting reaction mixture was heated to reflux with stirring for 7 d. After this period, the reaction mixture was cooled to room temperature and the solvent was evaporated to dryness under reduced pressure. The crude residue was taken up with ethyl acetate (10 mL) and placed in a refrigerator. The solid that precipitated on standing in the refrigerator was collected by Buchner filtration and then dissolved in dichloromethane (50 mL). The resulting solution was treated with 5 mL of trifluoroacetic acid and stirred at room temperature for 3 h. After this period, the solvent was evaporated to dryness under reduced pressure to afford dumbbells **DB-Short** and **DB-Long**.

DB-Short: (60%) ^1H NMR (400 MHz, CD_3OD): $\delta=1.31$ (s, 18H), 1.4–1.6 (m, 14H), 1.6 (brs, 2H), 1.7 (brs, 4H), 2.0 (brs, 2H), 2.1 (brs, 2H), 2.33 (s, 3H), 3.0 (brs, 4H), 3.97 (t, $J=6$ Hz, 2H), 4.16 (t, $J=6$ Hz, 2H), 4.67 (t, $J=7.6$ Hz, 2H), 4.77 (t, $J=7.6$ Hz, 2H), 5.08 (s, 1H), 6.75 (s, 2H), 7.03 (s, 1H), 7.2–7.3 (m, 12H), 7.69 (d, $J=8$ Hz, 2H), 8.64 (d, $J=6$ Hz, 4H), 9.22 (d, $J=6$ Hz, 2H), 9.28 ppm (d, $J=6$ Hz, 2H); ^{13}C NMR (100 MHz, CD_3OD): $\delta=20.0, 24.8, 25.1, 25.2, 25.4$ (2 res.), 25.8, 25.9, 27.9, 28.9, 30.5, 30.7, 30.9, 34.4, 56.9, 61.6, 61.7, 64.5, 67.2, 108.6, 114.4, 125.5, 126.9, 128.2, 128.3, 128.6, 138.9, 140.4, 142.3, 145.6, 145.7, 149.8, 149.9, 151.9, 158.8, 172.9 ppm; ESI-MS(+) m/z (%) [ion]: 839 (100) $[\text{M}-\text{H}]^+$.

DB-Long: (55%) ^1H NMR (400 MHz, CD_3OD): $\delta=1.31$ (s, 18H), 1.4–1.5 (m, 36H), 1.7 (brs, 4H), 1.8 (brs, 2H), 2.0 (brs, 2H), 2.1 (brs, 2H), 2.36 (s, 3H), 2.97 (t, $J=8$ Hz, 4H), 3.97 (t, $J=6.4$ Hz, 2H), 4.17 (t, $J=6.4$ Hz, 2H), 4.68 (t, $J=7.2$ Hz, 2H), 4.74 (t, $J=7.2$ Hz, 2H), 5.08 (s, 1H), 6.74 (s, 2H), 7.02 (s, 1H), 7.2–7.4 (m, 12H), 7.69 (d, $J=$

8 Hz, 2H), 8.65 (d, $J=6$ Hz, 4H), 9.22 (d, $J=6$ Hz, 2H), 9.26 ppm (d, $J=6$ Hz, 2H); ^{13}C NMR (100 MHz, CD_3OD): $\delta=20.0, 24.8, 25.1, 25.8, 25.9, 26.2, 27.8, 28.8$ (3 res.), 29.0, 29.1, 29.2 (2 res.), 30.5, 30.9, 31.2, 34.4, 56.9, 61.7, 61.9, 64.5, 67.5, 108.6, 114.3, 125.5, 126.9, 128.2, 128.3, 128.5, 138.9, 140.4, 145.7, 149.9 (2 res.), 151.8, 158.8, 172.9 ppm; ESI-MS(+) m/z (%) [ion]: 993 (100) $[\text{M}-\text{H}]^+$.

Electrochemical measurements and simulation

Cyclic voltammetric (CV) experiments were carried out at room temperature in argon-purged acetonitrile or acetone with an Autolab 30 multipurpose instrument interfaced to a PC by using a glassy carbon as working electrode, a Pt wire as counter electrode, and an Ag wire as quasireference electrode. The oxidation wave of ferrocene [$E_{1/2}(\text{Fc}^+/\text{Fc})=+0.395$ vs. SCE], added as a standard, was used to calibrate the potential scale and assess electrochemical reversibility. The concentration of the compounds examined was in the range 2×10^{-4} M to 4×10^{-4} M, and 0.04 M tetraethylammonium hexafluorophosphate was used as supporting electrolyte. Scan rates varying typically from 50 to 1000 mVs^{-1} were utilized. Differential pulse voltammetry (DPV) was performed with a scan rate of 20 mVs^{-1} , a pulse height of 75 mV, and a duration of 40 ms. For reversible processes the same half-wave potential values were obtained from the DPV peaks and from an average of the cathodic and anodic CV peaks. The potential values for processes that were not fully reversible were estimated from the DPV peaks. The experimental error in the potential values was estimated to be ± 10 and ± 20 mV, respectively. Digital fitting of the experimental CV for the **R-UpShort** system was obtained on the basis of the square-scheme mechanism illustrated in Figure 5 by using the software package DigiSim 3.05.^[48] The redox potentials were fixed in the simulation, and the shuttling equilibrium constant in the monoreduced form was fixed to 10; shuttling rate constants were optimized in the simulation. A value of 1 cm s^{-1} , representative of a reversible process under our conditions, was employed for the electron transfer rates.^[49] The charge-transfer coefficients were taken as 0.5 in all cases.

EPR measurements

EPR spectra were recorded at room temperature with an ELEXYS E500 spectrometer equipped with an NMR gaussmeter for the calibration of the magnetic field and a frequency counter for the determination of g factors, which were corrected against that of the perylene radical cation in concentrated sulfuric acid ($g=2.002583$). The electrochemical cell was homemade and consisted of an EPR flat cell (Wilma WG-810) equipped with a $25 \times 5 \times 0.2$ mm platinum gauze (cathode), and a platinum wire (anode).^[50,51] The current was supplied and controlled by an AMEL 2051 general-purpose potentiostat. In a typical experiment, the cell was filled with an acetonitrile solution of the appropriate substrate (ca. 1 mM) containing tetrabutylammonium perchlorate (ca. 0.1 M) as supporting electrolyte. After thoroughly purging the solution with N_2 , spectra were recorded at different potential settings in the range 0 to -0.8 V. An iterative least-squares fitting procedure based on the systematic application of the Monte Carlo method was performed to obtain the experimental spectral parameters of the radical species.^[52]

Acknowledgements

The authors thank Centro Interdipartimentale di Misura of the University of Parma for NMR and MS measurements. This work

was supported by the Italian MIUR (PRIN 2010CX2TLM) and the Universities of Parma and Bologna (FARB SLaMM project).

Conflict of interest

The authors declare no conflict of interest.

Keywords: calixarenes · electrochemistry · molecular devices · rotaxanes · supramolecular chemistry

- [1] S. Kassem, T. van Leeuwen, A. S. Lubbe, M. R. Wilson, B. L. Feringa, D. A. Leigh, *Chem. Soc. Rev.* **2017**, *46*, 2592–2621.
- [2] S. Silvi, M. Venturi, A. Credi, *J. Mater. Chem.* **2009**, *19*, 2279.
- [3] W. R. Browne, B. L. Feringa, *Nat. Nanotechnol.* **2006**, *1*, 25–35.
- [4] S. Erbas-Cakmak, D. A. Leigh, C. T. McTernan, A. L. Nussbaumer, *Chem. Rev.* **2015**, *115*, 10081–10206.
- [5] B. L. Feringa, W. R. Browne, *Molecular Switches*, Wiley-VCH, **2011**.
- [6] P. L. Anelli, N. Spencer, J. F. Stoddart, *J. Am. Chem. Soc.* **1991**, *113*, 5131–5133.
- [7] A. P. de Silva, I. M. Dixon, H. Q. N. Gunaratne, T. Gunnlaugsson, P. R. S. Maxwell, T. E. Rice, *J. Am. Chem. Soc.* **1999**, *121*, 1393–1394.
- [8] I. Willner, B. Basnar, B. Willner, *Adv. Funct. Mater.* **2007**, *17*, 702–717.
- [9] H. Hess, J. Clemmens, D. Qin, J. Howard, V. Vogel, *Nano Lett.* **2001**, *1*, 235–239.
- [10] J. Berná, D. A. Leigh, M. Lubomska, S. M. Mendoza, E. M. Pérez, P. Rudolf, G. Teobaldi, F. Zerbetto, *Nat. Mater.* **2005**, *4*, 704–710.
- [11] C. J. Bruns, J. F. Stoddart, *The Nature of the Mechanical Bond: From Molecules to Machines*, Wiley, **2016**.
- [12] T. Ogoshi, D. Yamafuji, T. Aoki, T. Yamagishi, *Chem. Commun.* **2012**, *48*, 6842.
- [13] A. Caballero, L. Swan, F. Zapata, P. D. Beer, *Angew. Chem. Int. Ed.* **2014**, *53*, 11854–11858; *Angew. Chem.* **2014**, *126*, 12048–12052.
- [14] E. M. Lewis, M. Galli, S. M. Goldup, *Chem. Commun.* **2017**, *53*, 298.
- [15] A. Altieri, F. G. Gatti, E. R. Kay, D. A. Leigh, D. Martel, F. Paolucci, A. M. Z. Slawin, J. K. Y. Wong, *J. Am. Chem. Soc.* **2003**, *125*, 8644–8654.
- [16] A. M. Brouwer, C. Frochot, F. G. Gatti, D. A. Leigh, L. Mottier, F. Paolucci, S. Roffia, G. W. H. Worpel, *Science* **2001**, *291*, 2124–2128.
- [17] a) V. Balzani, A. Credi, M. Venturi, *Chem. Soc. Rev.* **2009**, *38*, 1542–50; b) V. Balzani, A. Credi, M. Clemente-León, B. Ferrer, M. Venturi, A. H. Flood, J. F. Stoddart, *Proc. Natl. Acad. Sci. USA* **2006**, *103*, 1178–1186.
- [18] a) P. R. Ashton, R. Ballardini, V. Balzani, I. Baxter, A. Credi, M. C. T. Fyfe, M. T. Gandolfi, M. Gómez-López, M.-V. Martínez-Díaz, A. Piersanti, N. Spencer, J. F. Stoddart, M. Venturi, A. J. P. White, D. J. Williams, *J. Am. Chem. Soc.* **1998**, *120*, 11932–11942; b) S. Erbas-Cakmak, S. D. P. Fielden, U. Karaca, D. A. Leigh, C. T. McTernan, D. J. Tetlow, M. R. Wilson, *Science* **2017**, *358*, 340–343.
- [19] G. Ragazzon, M. Baroncini, S. Silvi, M. Venturi, A. Credi, *Nat. Nanotechnol.* **2015**, *10*, 70–75.
- [20] J. V. Hernández, E. R. Kay, D. A. Leigh, *Science* **2004**, *306*, 1532–1537.
- [21] M. von Delius, E. M. Geertsema, D. A. Leigh, *Nat. Chem.* **2010**, *2*, 96–101.
- [22] D. A. Leigh, J. K. Y. Wong, F. Dehez, F. Zerbetto, *Nature* **2003**, *424*, 174–179.
- [23] C. Casati, P. Franchi, R. Pievo, E. Mezzina, M. Lucarini, *J. Am. Chem. Soc.* **2012**, *134*, 19108–19117.
- [24] P. Waelès, K. Fournel-Marotte, F. Coutrot, *Chem. Eur. J.* **2017**, *23*, 11529–11539.
- [25] R. A. Bissell, E. Córdoba, A. E. Kaifer, J. F. Stoddart, *Nature* **1994**, *369*, 133–137.
- [26] T. Oshikiri, Y. Takashima, H. Yamaguchi, A. Harada, *J. Am. Chem. Soc.* **2005**, *127*, 12186–12187.
- [27] J. W. Park, H. J. Song, *Org. Lett.* **2004**, *6*, 4869–4872.
- [28] a) C. Talotta, C. Gaeta, P. Neri, *Org. Lett.* **2012**, *14*, 3104–3107; b) T. Pierro, C. Gaeta, C. Talotta, A. Casapullo, P. Neri, *Org. Lett.* **2011**, *13*, 2650; c) R. Cio, C. Talotta, C. Gaeta, L. Margarucci, A. Casapullo, P. Neri, *Org. Lett.* **2013**, *15*, 5694–5697.
- [29] H.-X. Wang, Z. Meng, J.-F. Xiang, Y.-X. Xia, Y. Sun, S.-Z. Hu, H. Chen, J. Yao, C.-F. Chen, *Chem. Sci.* **2016**, *7*, 469–474.
- [30] T. Oshikiri, H. Yamaguchi, Y. Takashima, A. Harada, *Chem. Commun.* **2009**, *0*, 5515.
- [31] A. Arduini, R. Bussolati, A. Credi, S. Monaco, A. Secchi, S. Silvi, M. Venturi, *Chem. Eur. J.* **2012**, *18*, 16203–16213.
- [32] A. Arduini, R. Bussolati, A. Credi, A. Pochini, A. Secchi, S. Silvi, M. Venturi, *Tetrahedron* **2008**, *64*, 8279–8286.
- [33] V. Zanichelli, G. Ragazzon, A. Arduini, A. Credi, P. Franchi, G. Orlandini, M. Venturi, M. Lucarini, A. Secchi, S. Silvi, *Eur. J. Org. Chem.* **2016**, 1033–1042.
- [34] A. Credi, S. Dumas, S. Silvi, M. Venturi, A. Arduini, A. Pochini, A. Secchi, *J. Org. Chem.* **2004**, *69*, 5881–5887.
- [35] A. Arduini, F. Calzavacca, A. Pochini, A. Secchi, *Chem. Eur. J. Chem.-A Eur. J.* **2003**, *9*, 793–799.
- [36] A. Arduini, F. Ciesca, M. Fragassi, A. Pochini, A. Secchi, *Angew. Chem. Int. Ed.* **2005**, *44*, 278–281; *Angew. Chem.* **2005**, *117*, 282–285.
- [37] G. Orlandini, G. Ragazzon, V. Zanichelli, A. Secchi, S. Silvi, M. Venturi, A. Arduini, A. Credi, *Chem. Commun.* **2017**, *53*, 6172–6174.
- [38] V. Zanichelli, G. Ragazzon, G. Orlandini, M. Venturi, A. Credi, S. Silvi, A. Arduini, A. Secchi, *Org. Biomol. Chem.* **2017**, *15*, 6753–6763.
- [39] A. Arduini, R. Ferdani, A. Pochini, A. Secchi, F. Ugozzoli, *Angew. Chem. Int. Ed.* **2000**, *39*, 3453–3456; *Angew. Chem.* **2000**, *112*, 3595–3598.
- [40] A. Arduini, R. Bussolati, A. Credi, A. Secchi, S. Silvi, M. Semeraro, M. Venturi, *J. Am. Chem. Soc.* **2013**, *135*, 9924–9930.
- [41] M. Semeraro, A. Arduini, M. Baroncini, R. Battelli, A. Credi, M. Venturi, A. Pochini, A. Secchi, S. Silvi, *Chem. Eur. J.* **2010**, *16*, 3467–3475.
- [42] R. Ballardini, A. Credi, M. T. Gandolfi, C. Giansante, G. Marconi, S. Silvi, M. Venturi, *Inorganica Chim. Acta* **2007**, *360*, 1072–1082.
- [43] A. Arduini, R. Bussolati, A. Credi, G. Faimani, S. Garaudée, A. Pochini, A. Secchi, M. Semeraro, S. Silvi, M. Venturi, *Chem. Eur. J.* **2009**, *15*, 3230–3242.
- [44] T. Belser, M. Stöhr, A. Pfaltz, *J. Am. Chem. Soc.* **2005**, *127*, 8720–8731.
- [45] M. Yoritake, T. Meguro, N. Matsuo, K. Shirokane, T. Sato, N. Chida, *Chem. Eur. J.* **2014**, *20*, 8210–8216.
- [46] A. Boccia, V. Lanzilotto, V. Di Castro, R. Zanon, L. Pescatori, A. Arduini, A. Secchi, *Phys. Chem. Chem. Phys.* **2011**, *13*, 4452–4462.
- [47] J. J. González, R. Ferdani, E. Albertini, J. M. Blasco, A. Arduini, A. Pochini, P. Prados, J. de Mendoza, *Chem. Eur. J.* **2000**, *6*, 73–80.
- [48] DigiSim 3.05, BioAnalytical Systems, West Lafayette, IN, see: www.bioanalytical.com.
- [49] A. J. Bard, L. R. Faulkner, *Electrochemical Methods, Fundamentals and Applications*, Wiley, New York, **1980**, Chapter 6.
- [50] A. Alberti, M. Benaglia, P. Hapiot, A. Hudson, G. Le Coustumer, D. Maciantelli, S. Masson, *J. Chem. Soc. Perkin Trans. 2* **2000**, 1908–1913.
- [51] C. Boga, M. Calvaresi, P. Franchi, M. Lucarini, S. Fazzini, D. Spinelli, D. Tonelli, *Org. Biomol. Chem.* **2012**, *10*, 7986–7995.
- [52] P. Franchi, E. Mezzina, M. Lucarini, *J. Am. Chem. Soc.* **2014**, *136*, 1250–1252.

Manuscript received: January 31, 2018

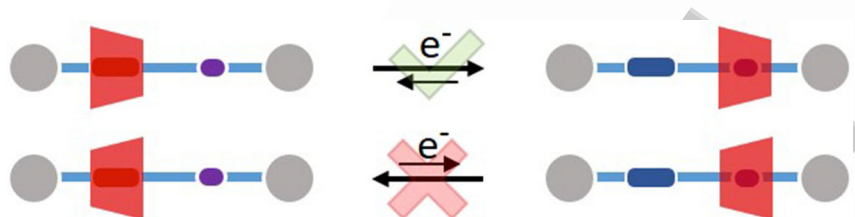
Accepted manuscript online: April 16, 2018

Version of record online: ■ ■ ■ 0000

FULL PAPER

Molecular Machines

V. Zanichelli, M. Bazzoni, A. Arduini,
P. Franchi, M. Lucarini, G. Ragazzon,*
A. Secchi,* S. Silvi*

Redox-Switchable Calix[6]arene-Based
Isomeric Rotaxanes

One-way rotaxanes: A series of isomeric redox-switchable calix[6]arene-based rotaxanes were synthesized by a reagent-less strategy. It was demonstrated

that the orientation of the calix[6]arene wheel can give rise to a thermodynamic preference for shuttling among orientational isomers (see figure).



Isomeric, redox-switchable, calixarene-based, two-station #rotaxanes @unipr @UniPadova **SPACE RESERVED**
FOR IMAGE AND LINK

Share your work on social media! *Chemistry - A European Journal* has added Twitter as a means to promote your article. Twitter is an online microblogging service that enables its users to send and read text-based messages of up to 140 characters, known as “tweets”. Please check the pre-written tweet in the galley proofs for accuracy. Should you or your institute have a Twitter account, please let us know the appropriate username (i.e., @accountname), and we will do our best to include this information in the tweet. This tweet will be posted to the journal’s Twitter account @ChemEurJ (follow us!) upon online publication of your article, and we recommended you to repost (“retweet”) it to alert other researchers about your publication.

Please check that the ORCID identifiers listed below are correct. We encourage all authors to provide an ORCID identifier for each coauthor. ORCID is a registry that provides researchers with a unique digital identifier. Some funding agencies recommend or even require the inclusion of ORCID IDs in all published articles, and authors should consult their funding agency guidelines for details. Registration is easy and free; for further information, see <http://orcid.org/>.

Dr. Valeria Zanichelli <http://orcid.org/0000-0003-2642-1578>

Margherita Bazzoni <http://orcid.org/0000-0002-4701-6267>

Prof. Arturo Arduini <http://orcid.org/0000-0003-2774-0095>

Dr. Paola Franchi <http://orcid.org/0000-0001-5469-1941>

Prof. Marco Lucarini <http://orcid.org/0000-0002-8978-4707>

Dr. Giulio Ragazzon <http://orcid.org/0000-0002-7183-2985>

Prof. Andrea Secchi <http://orcid.org/0000-0003-4045-961X>

Dr. Serena Silvi <http://orcid.org/0000-0001-9273-4148>